Lagrangian cloud microphysics models use relatively few computational droplets (also known as super-droplets, SDs) to represent huge number of real droplets that clouds are made of. This simplification makes it difficult to model coalescence of droplets and artificially amplifies fluctuations associated with transport and coalescence. The paper presents a novel method of mitigating these issues and is of potential interest for the GMD readers. The method proposed is to split computational droplets that represent large fraction of liquid water into couple computational droplets, each representing a smaller amount of liquid water. This new approach is shown to improve results of simulations, especially in the idealized box models. However, some non-trivial results are only vaguely discussed, or their analysis is arbitrary. Therefore I suggest including a more detailed discussion of the results, that would address the following points:

First of all, we would like to thank the reviewer for the detailed and constructive feedback. With the help of this review, we hope to have considered all missing points and open questions in the revised version.

1. Single cloud simulations of cumulus show, that splitting increases the amount of rain water. This increase is not seen in the cloud field simulation. Authors conclude that there is no increase in rain water because of averaging over a large cloud field (p.15 l.4). I do not understand how this is relevant. If amount of rain water in each cloud is increased, the average should also be increased.
Author's answer: This objection is correct. As you suggested in the next comment we ran for each of the reference simulations a small ensemble (for each case 5 ensembles), showing that differences in the RWP and Z can be lead back to different model realizations. In the revised manuscript in Fig. 15 (in former revision Fig. 13) for each case one model realizations is shown as well the range of the different model realizations.
Modification (Ensembles of single cloud): ~~All splitting configurations show higher RWPs in comparison to the reference runs without splitting.This increase of up to 12% is a direct result of the improved collisional growth process in the splitting configurations, resulting in more numerous and larger rain drops.This is also observed for the radar reflectivity (Fig. 11d), which is proportional to the second moment of the DSD and hence more sensitive to larger droplets.~~

In the reference simulations (represented as a mean of 5 ensemble for each case) of Figs. 15c and 15d, one can seen an increase in the precipitation parameters (RWP, radar reflectivity and precipitation sum) for an increased number of superdroplets. However, the differences among the ensembles members are quite large, which is

shown by the range (gray area) and the band of plus-minus one standard deviation from the mean (light blue area) derived from all 15 ensemble members. Overall, the splitting simulations have a slight tendency to compare better with the reference cases using 87 and 186 superdroplets. Admittedly, since the results are (for the most part) within one standard deviation, it can be concluded that splitting has no significant influence on the global precipitation parameters.

(**page 14 line 14)**

[...]

Considering the temporal variability of the precipitation rate and total precipitation (Fig. 17e and f), no significant changes are detectable using splitting or a very high number of superdroplets ~~in contrast to the single cloud simulations presented in the last section~~. ~~This is foremost a result of the larger model domain alone, which attenuates variability simply by averaging.~~ (**page 16 line1)**

[...]

In the idealized single cloud simulation, splitting improved the representation of collisional growth with up to 70 % larger maximum radii ~~and a slight increase of the rain water path of up to 12 %~~.

(page 16 line 31)

[...]

Figure 15: Ensemble results added.

Timeseries of different variables for the idealized single cloud simulation for different initial numbers of superdroplets and splitting configurations. In (a), the ratio of the actual and initialized number of superdroplets in the whole model domain is shown. The liquid water path (LWP) and rainwater path (RWP) are displayed in panels (b) and (c), respectively. In (d), the total radar reflectivity is shown. Panels (e) and (f) show the precipitation rate and total precipitation, respectively. The reference simulations (runs without splitting) are presented as a mean of five ensembles for each case. Moreover, the light blue areas show the mean plus-minus one standard deviation and the gray areas show the range derived from all 15 ensemble members.

2. Judging from single cloud simulations, merging increases radar reflectivity and amount of precipitation (see Fig. 13, especially for the S20 case). I suppose that this is not the case, but that the difference comes from different model realizations. This could be clarified if a small ensemble of single cloud simulations was ran for each case discussed in the section 4.2.
Author's answer: As mentioned above, we agree with this comment and have adapted our manuscript (see comment above).
Modification: The extensive changes and results of the ensemble runs are summarized in the response to the first comment to which reference is made here.

3. In single cloud simulations without splitting, amount of precipitation decreases as the number of computational droplets is increased (Fig. 13). Simulations with splitting are in better agreement with N_p= 15 than with Np= 186 .Why is it so?
Author's answer: This expression occurred due to using only one model realization. Different realizations show different results which are now considered in Fig. 15 (old Fig. 13).
Modification: The extensive changes and results of the ensemble runs are summarized in the response to the first comment above.

4. In box model simulations without splitting, largest droplets produced in LCM are larger than the Smoluchowski equation predicts, especially if number of computational particles is large (Fig. 5). On page 9, line 26, Authors argue that this is because there are few large SDs with high weighting factors. If this is the case, then shouldn't the effect decrease with increasing number of SDs? The opposite is observed - this effect is more pronounced as more SDs are added. Moreover, if the Authors' argument was correct, splitting of SDs should also fix this problem. On the contrary, LCM with splitting also produces too large droplets, as seen in Figs. 7 and 10.
Author's answer: The underlying problem here is the initialization, which cannot be fixed by splitting. The initialization with constant weighting factors will always deviate from the exponential initialization used by Wang et al. (2007). Therefore, subsequent collisions, which are improved by splitting, cannot agree with the bin-solution by Wang et al. (2007) whatsoever. Thus, the decreasing difference among the different LCM simulations, as it is occurring due to splitting, needs to be seen as a proof of concept, and not the comparison with the bin results.

Modification (**page 11 line 2):** Again, general differences between the models are caused by the (problematic) initialization, which cannot be fixed by splitting. The initialization with constant weighting factors will always deviate from the exponential initialization used by Wang et al. (2007). Therefore, subsequent collisions, which are improved by splitting, cannot agree with the bin-solution by Wang et al. (2007) whatsoever. Thus, the decreasing difference among the different LCM simulations, as it is occurring due to splitting, needs to be seen as a proof of concept, and not the comparison with the bin results.

5. In the first paragraph of "Conclusions", Authors claim that LCMs are "known to insufficiently represent" coalescence. I suppose that they are referring to results of box model simulations, shown in Fig. 1. Not all LCM insufficiently represent coalescence, but only those that initialize SDs in the same way it is done in the paper. Other initialization procedures give much better box model results, e.g. Dziekan and Pawlowska 2017.

Author's answer: Sorry for this misunderstanding. This statement is based on the insufficient representation of collision/coalescence in LCMs with a constant weighting factor, which is a typical way to initialize those models in three-dimensional applications. We definitely agree that LCMs with different initialization methods are able to represent collision very well (e.g. in box models) even without splitting. However, in three-dimensional applications, it is not always possible to use such initialization methods (like singleSIP or multiSIP).

Modification (page 16 line 12): These models are able to represent collision and coalescence well (Unterstrasser et al., 2017;Dziekan and Pawlowska, 2017). Under certain conditions, however, they are known to insufficiently represented this process.

These conditions occur when the number of superdroplets is low and, accordingly, the number of real droplets represented by each superdroplet (the so-called weighting factor) is high, leading to an oversimplified representation of the droplet size distribution (DSD) (Riechelmann et al., 2012; Unterstrasser et al., 2017).

[...]

examples for LCM applications using a constant weighting factor/multiplicity (e.g. Shima et al., 2009; Riechelmann et al., 2012; Arabas and Shima, 2013; Naumann and Seifert, 2015, Hoffmann et al., 2017; Sardina et al., 2018) **(page 7 line 15)**

6. In "Conclusions", cloud field simulations are claimed to show similar effects of splitting on the production of rain as single cloud simulations. This is not true -

splitting increases the amount of rain in single cloud simulations, but does not affect the amount of rain in cloud field simulations.
Author's answer: The ensembles show that our conclusion to macrophysical properties of a single cloud was not correct. We corrected that in the revised revision. Now it is in accordance that splitting does not change cloud-wide properties as rain water path or radar reflectivity, but has an influence on the spatial and temporal representation of rain droplets and the representation of the DSD.
Modification: The extensive changes and results of the ensemble runs are summarized in the response to the first comment to which reference is made here.

7. A short discussion of potential impact of SD merging on aerosol processing would be desirable.
Author's answer: Merging needs and can be adopted for future applications in which aerosol size and composition are considered. However, these more sophisticated approaches are not in the scope of the presented paper which focuses on the production of rain.
Modification (SD merging on aerosol processing): Furthermore, it must be mentioned that the merging algorithm described here, do not conserve size and chemical composition of the aerosol. Therefore, studies that explicitly simulate the activation process may have to adapt the merging algorithm. **(page 6 line 25)**

8. Authors write that merging of SDs reduces computing time by 18% . How does splitting affect performance?
Author's answer: A short answer is: the computing time increases about 0-20% depending on how many particles are created (for the idealized cloud setup). We observed that the simulation S20 requires 19.2% more computing time than the reference simulation const. N_p87. By applying splitting, the simulation S20 merging had nearly the same computational time than the reference simulation and was only 1.2% slower.
The storage demand can be estimated from Fig. 13a. The ratio of the actual number of superdroplets to the initialized number of superdroplets is a measure of the increased demand, where the highest increase can be observed at S10 which is about 15%.
Modification (page 15 line 3): To estimate the increase in computing time due to splitting, we conducted three simulations (const. N_P87, S20 and S20merging) with comparable time measurements. The constraint to three simulations is caused by a special mode which is required for time measurements on the supercomputer but

leads to an increase in computing time. Here, we observe that a splitting-simulation S20 require 19.2% more computing time than the reference simulation const. N_P87. If applied, merging allows a massive reduction of the number of superdroplets, reducing the computing time by 18% and the storage demand (which is proportional to the number of superdroplets) by at least by 7% compared to simulations applying only splitting (Fig.13a). All in all, the simulation applying both splitting and merging, is only 1.2% slower than the reference simulation const. N_P 87.

Technical comments:

9. In lower panels of Fig. 15, precipitation rate from vanZanten et al. 2011 should be shown.

Author's answer: The precipitation rate is added in the revised version.

Modification (Figure 15): The precipitation rate from vanZanten et al. 2011 is added.

10. Through the paper, large variability in results is alternatively called "oscillations" or "fluctuations" (e.g. p. 8, l. 19). Oscillation is a periodic process, so I suggest the word "fluctuations" to be used.

Author's answer: This is corrected in the revised version.

Modification (page 9 line 11 and page 9 line 27): “oscillations” → “fluctuations”

11. In the last line on page 3, Authors write that splitting makes their approach "fundamentally different". To me this seems to be a too strong statement - "different" would suffice.

Author's answer: This is corrected in the revised version.

Modification (page 4 line 3): [..]~~fundamentally~~ different[..]

12. Why is the blue line in Fig. 16 discontinuous?

Author's answer: To calculate the PDF of the precipitation rate, the rates were discretized. With a low number of superdroplets, some bins are empty due to a lack of statistics, which explains the discontinuity of the function.

13. In Fig. 5 spectra for 512 and 1000 SDs have a local maximum on the large end. What is the cause?

Author's answer: A closer analysis reveals this also the case with 15 and 37 superdroplets. The reason for this is the insufficient statistics (even with 500 and 1000 superdroplets per grid box) in the range of very large drops. The data shows

1 Introduction

The authors introduce a new extension of the lagrangian microphysics schemes- the splitting and merging algorithm. The splitting part of the algorithm increases the resolution of the lagrangian microphysics scheme for big droplets. This is especially important for correctly representing the collisions between droplets and the resulting onset of precipitation. The merging part of the algorithm decreases slightly the computational cost of the splitting algorithm. Both developments are described and tested. The paper is well written and interesting for the GMD community. It should be published after some corrections and additional tests.

First of all, we would like to thank the reviewer for the detailed and constructive feedback. With the help of this review we hope to have considered all missing points and open questions.

2 Major comments

• A lagrangian microphysics scheme can represent collisions in different ways and can be initialized in different ways. Both choices have big impact on the accuracy of the scheme, Unterstrasser et al. (2017). Here the authors in their implementation of the lagrangian microphysics scheme use the most accurate way to represent collisions (the all-or-nothing algorithm Shima et al. (2009)). This is great. However, they initialize the droplet size distribution with constant weighting factors. This is the worst initialization strategy for representing collisions, see Figure 1 in Unterstrasser et al. (2017). It cannot be said that this is the standard way to initialize lagrangian microphysics schemes. Other groups initialize their schemes in different ways, see for example Unterstrasser and Sölch (2014), Arabas et al. (2015). Because this work focuses on improving the representation of collisions between droplets, such a bad-for-collisions initialization choice is not justifiable. The authors should also test their splitting and merging algorithm with a better initialization way (any of the singleSIP, multiSIP or v random from Unterstrasser et al.(2017) would suffice). Redoing the single cloud and cloud field simulations might be to expensive and unnecessary for the purpose of testing. However, it would be very interesting to see the single and multi-box tests done again with a different initialization choice. Does the splitting and merging algorithm improve the results as much for a different initialization choice Are the multi-box simulations really necessary if the droplet size distribution is initialized correctly? How does the estimate given in line 25 on page 15 change with a better initialization?

Author's answer: That objection is correct. We already performed single-box simulations with singleSIP initialization to validate our collision algorithm. These simulations show that we achieve very good results with 87 particles per grid box compared to

the bin model. For this initialization, splitting only results in a slight reduction of fluctuations compared to simulations with a small number of superdroplets. However, as described in the paper, in real 3D applications, as with an idealized box model, it is not guaranteed that large drops (relevant as collision embryos) are statistically sufficiently represented. In fact, many 3D LCM applications use the same weighting factor for all superdroplets in their simulations, which we tried to mimic in our box simulations.

Modification (concerning different initialization): As reference, the singleSIP initialization of Unterstrasser et al. (2017) is used for the single-box model, too. In contrast to the previously described initialization, the initial DSD is discretized using logarithmically spaced bins. The number of bins corresponds to the number of superdroplets. To each bin, a superdroplet with a corresponding mean radius and weighting factor is assigned. The maximum radius of the initial distribution is approximately 33 μm, which corresponds to a number of concentrations of $1/\Delta V$. This avoids superdroplets with a weighting factor less than 1. Note that this (not always applicable) initialization technique represents the inherent variability of droplet radii and their abundance across the initial spectrum much more accurately than the previously described method, and, therefore results in a much better agreement with literature
references. **(page 8 line 6)**
[...]
Figures 1 and 2 show the mass density distribution after 3600 s and the temporal development of the moments for the LCM applied as a single-box model using the singleSIP initialization by Unterstrasser et al. (2017). Each grid box is initialized with a different number of superdroplets (colored lines). The reference solution of Wang et al. (2007) is shown as a black solid line. Figure 1 shows that even with 87 superdroplets the solution of Wang et al. (2007) can be reproduced well and a further increase
in the number of superdroplets only leads to minor improvements. The small deviations between the bin model solution and the LCM can be traced back to the different solution of the collection equation (e.g., Dziekan and Pawlowska, 2017). Overall, it can be seen that the solution of the LCM converges with an increasing number of superdroplets. The moments of mass distribution (Fig. 2) also show convergence with an increasing number of superdroplets. This good representation of collision growth is in line with the results with Unterstrasser et al. (2017).
Now, Figs. 3 and 4 show the same quantities but for the initialization with identical weighting factors.
(page 8 line 29)

• **page 6 line 3:** What is more important in counterbalancing the increase in super-droplet number due splitting algorithm? - Is it the limiting number of super-droplet per grid-box $N_{P,max}$ or merging algorithm? What is the impact of merging on the possible future activation of merged super-droplets to cloud droplets? What is the resulting resolution of the scheme for aerosol particles after merging? Is merging more accurate than using super-droplets just for representing clouds and precipitation and parameterizing activation process, as it is done in Grabowski et al. (2018)?
Author's answer: Both, the merging algorithm and the limitation of the number of superdroplets, are very important mechanisms to keep the number of superdroplets at a computationally feasible level. However, they work in different places. $N_{P,max}$ limits the number of superdroplets of a grid box inside the cloud, which is necessary to compute collisions in a reasonable amount of time (the performance of the collision algorithm is O(N^2)). Merging, on the other hand, nudges the superdroplet concentration outside the cloud to the initial superdroplet concentration. Overall, $N_{P,max}$ is a necessary constraint to be able to perform the simulation with splitting, while merging is a good supplement to save computing time.

In this study, the explicit representation of activation (which is a strength of LCMs) was neglected. At present, the merging algorithm would not take into account the size and chemical composition of aerosols. Although certain additions to the merging algorithm to cope with the size and chemical composition of aerosols are imaginable, they are out of the scope of the is manuscript.

In contrast to the approach of Grabowski et al. (2018), our approach would allow to track detailed changes in the number (and, in possible future applications, the size and composition) of aerosols. In that sense, merging is more accurate but needs more computing time and memory since the baseline number of superdroplets is higher.

Modification (page 6 line 19): See modifications to next comment and comment concerning "page 15 line 27".

• **page 6 line 16-19:** The mass conservation is a necessary constraint. But it is not enough to determine the super-droplet properties after merging. For the purpose of this study it's probably not important to have a more detailed strategy for determining super-droplet properties after merging. However it might be important for aerosol processing or secondary activation of aerosol particles to cloud droplets.
Having that in mind, what would be the best way to determine the super-droplet properties after merging? For example: The current one assumes that the super-droplet radius

after merging is equal to the radius of the super-droplet with the bigger weighting factor. An alternative could be to assume that the weighting factors are summed and to calculate the new radius from the mass conservation?

Author's answer: Thanks for that suggestion, we also did this. Furthermore, we merged the two most similar superdroplets, summing both weighting factors, and as you suggested, calculate the new radius. However, the results shows no difference to the current method except that the actually applied algorithm is computationally more efficient, which is a strong cause for the usage of the proposed method.
Modification (page 6 line 19): Moreover, a more advanced method where the most similar droplets (within one grid box) concerning their mass are merged was tested. Using this, simulations shows that there are no indications for different results using the advanced method. However, due to a sorting process the computing time is increased in comparison to the simple method.
[…]
Furthermore, it must be mentioned that the merging algorithm described here, do not conserve size and chemical composition of the aerosol. Therefore, studies that explicitly simulate the activation process may have to adapt the merging algorithm. **(page 6 line 25)**

• **page 7 line 11:** Are all the boxes in the multi-box simulation homogeneous and there is no droplet sedimentation? If yes, what is the difference between the introduced here multi-box approach and a single-box simulation that would use a better way to initialize the droplet size distribution (with a better initial representation of the tail of the distribution) and use the same total number of super-droplets as the multi-box simulation? What is the total volume simulated in the multi-box approach vs the single-box? Is multi-box approach increasing the simulated volume only to introduce different realizations of the initial condition to counter the problems introduced by the constant weighting factor initialization?
Author's answer: Yes, in the multi-box approach droplet sedimentation is not considered. The multi-box approach is an attempt to represent collisional growth with an unfortunate initialization (limited number of superdroplets per grid box and (high) constant weighting factor) under idealized conditions (box model simulation, with initial size spectrum), while allowing superdroplets to move between grid boxes as in a three-dimensional simulation. Of course you are right an unfettered comparison between the single-box and multi-box approach is not fair.

And we agree that the multi-box approach increases the simulated volume by introducing different realizations of the initial conditions, which partly counters the problems introduced by the initialization with a constant weighting factor.
However, the relative differences are interesting. Seeing that in the multi-box approach splitting of the largest droplets is a powerful tool to mitigate a bad initialization and to represent the size droplet distribution is as good as it is with 1000 superdroplets (in the multi-box approach) initially.

When a different initialization is used (singleSIP from Unterstrasser et al (2017)), which is now displayed in Figs. 1 and 2, no splitting or multi-box approach is necessary to reach a high agreement with the bin reference. However, as shown in comment to page 7 line 6, initializing LCMs with a constant weighting factor is common in many LES-LCM applications.
Modification (page 7 line 11): Modifications to this comment are included in the changes related to the first comment of the reviewer (see first major comment).

• **Both the high super-droplet concentration simulations** (Fig 5) and the splitting simulations (Fig 7) overestimate the biggest droplet sizes. Why? Would using even more super-droplets allow to reach better agreement with the bin reference simulation for the biggest droplet sizes?
Author's answer: The underlying problem here is the initialization, which cannot be fixed by splitting. The initialization with constant weighting factors will always deviate from the exponential initialization used by Wang et al. (2007). Therefore, subsequent collisions, which are improved by splitting, cannot agree with the bin-solution by Wang et al. (2007) whatsoever. Thus, the decreasing difference among the different LCM simulations, as it is occurring due to splitting, needs to be seen as a proof of concept, and not the comparison with the bin results.
Modification (**page 11 line 2):** Again, general differences between the models are caused by the (problematic) initialization, which cannot be fixed by splitting. The initialization with constant weighting factors will always deviate from the exponential initialization used by Wang et al. (2007). Therefore, subsequent collisions, which are improved by splitting, cannot agree with the bin-solution by Wang et al. (2007) whatsoever. Thus, the decreasing difference among the different LCM simulations, as it is occurring due to splitting, needs to be seen as a proof of concept, and not the comparison with the bin results.

• **page 11 line 14:** What is the benefit of using a 3-dimensional simulation setup if the initial condition is 2-dimensional? Using a 2-dimensional setup (with cyclic boundary condition in the missing dimension) would reduce the computational

cost by two orders of magnitude. This in turn would allow to test the performance, accuracy and convergence of the scheme for two orders of magnitude higher super-droplet concentrations.
Author's answer: This setup was used because it is well known and extensively tested by our group (Riechelmann et al., 2012, Hoffmann et al., 2013, Hoffmann et al., 2017). We agree that a full three-dimensional cloud setup is more appropriate and we will switch to such a setup in the future. However, using a pure two-dimensional setup would lead to a different evolution of turbulence, even though this may be negligible in our study. Moreover, since the computing time increases quadratic with the number of superdroplets per grid box and the parallelization is done in vertical columns the estimation that a two-dimensional setup would allow by two orders of magnitude higher superdroplet concentrations is unfortunately not applicable to our model.

• **Figure 11:** I agree that eliminating the fluctuations in the size distribution of big droplets is a good result. However, the box model tests (Fig 5 and 7) show that the lagrangian scheme overestimates the sizes in the large tail of the droplet distribution. Therefore the fact that the biggest drop size for the simulation with splitting is 350µm bigger might not necessarily be an improvement?
Author's answer: Differences in the box-model simulation to the bin model are caused by the initialization (see comment to Fig. 5 and 7), which are specific to the box-simulations and the comparison with the bin-solution. Accordingly, the fact that the maximum droplet size is increased in more-dimensional simulations, should be seen as an improvement gained from the better representation of collision and coalescence.

• **Figure 11 and 12:** Is there any change in the behavior for the small droplet sizes at t=3000s (end of the simulation) that is caused by merging?
Author's answer: No, merging affects only superdroplets with radii smaller than 0.1 µm in non-cloudy regions. Accordingly, these particles contain too little water to affect any of the displayed quantities.

• **Figure 13 c, d, f:** Why is the simulation with the biggest initial concentration of super-droplets (N=186) the biggest outlier? Out of the simulations without splitting and merging I would expect the one with initial N=15 to perform the worst and not the best. If the resolution for big droplets is important for collisions then the N=186 simulation should be better than N=15? Would running an ensemble average help? Or is this behavior consistent for even higher initial super-droplet concentrations?

Author's answer: This objection is correct. We decided to run an ensemble for each reference simulations (5 simulations for each case). They show that differences in the RWP and Z can be traced back to different model realizations. In the revised manuscript (Fig. 15), we now show the ensemble mean and range of the different model realizations.

Modification (**Ensembles of single cloud):** ~~All splitting configurations show higher RWPs in comparison to the reference runs without splitting.This increase of up to 12% is a direct result of the improved collisional growth process in the splitting configurations, resulting in more numerous and larger rain drops.This is also observed for the radar reflectivity (Fig. 11d), which is proportional to the second moment of the DSD and hence more sensitive to larger droplets.~~

In the reference simulations (represented as a mean of 5 ensemble for each case) of Figs. 15c and 15d, one can seen an increase in the precipitation parameters (RWP, radar reflectivity and precipitation sum) for an increased number of superdroplets. However, the differences among the ensembles members are quite large, which is shown by the range (gray area) and the band of plus-minus one standard deviation from the mean (light blue area) derived from all 15 ensemble members. Overall, the splitting simulations have a slight tendency to compare better with the reference cases using 87 and 186 superdroplets. Admittedly, since the results are (for the most part) within one standard deviation, it can be concluded that splitting has no significant influence on the global precipitation parameters.

(**page 14 line 14)**

[...]

Considering the temporal variability of the precipitation rate and total precipitation (Fig. 17e and f), no significant changes are detectable using splitting or a very high number of superdroplets ~~in contrast to the single cloud simulations presented in the last section~~. ~~This is foremost a result of the larger model domain alone, which attenuates variability simply by averaging.~~ (**page 16 line1)**

[...]

In the idealized single cloud simulation, splitting improved the representation of collisional growth with up to 70 % larger maximum radii ~~and a slight increase of the rain water path of up to 12 %~~.

(page 16 line 31)

[...]

Figure 15: Ensemble results added.

Timeseries of different variables for the idealized single cloud simulation for different initial numbers of superdroplets and splitting configurations. In (a), the ratio of the actual and initialized number of superdroplets in the whole model domain is shown. The liquid water path (LWP) and rainwater path (RWP) are displayed in panels (b) and (c), respectively. In (d), the

total radar reflectivity is shown. Panels (e) and (f) show the precipitation rate and total precipitation, respectively. The reference simulations (runs without splitting) are presented as a mean of five ensembles for each case. Moreover, the light blue areas show the mean plus-minus one standard deviation and the gray areas show the range derived from all 15 ensemble members.

• **page 14 line 6:** What is the computational cost and storage demand increase due to splitting algorithm?
Author's answer: This question must be answered separately. A short answer is: the computing time increases about 0-20% in dependence of how many particles are created (for the idealized cloud setup). Here, we see that the simulation *S20* requires

19.2% more computational time than the reference simulation *const.* N_p87. By applying splitting the simulation *S20 merging* needed nearly the same computational time than the reference simulation and was only 1.2% slower.
The storage demand can be estimated from figure 13a. The ratio of the actual number of superdroplets to the the initialized number of superdroplets is a measure of the increased demand, where the highest increase can be observed for *S10* which is about 15%.
Modification (page 15 line 3): To estimate the increase in computing time due to splitting, we conducted three simulations (const. N_P87, S20 and S20merging) with comparable time measurements. The constraint to three simulations is caused by a special mode which is required for time measurements on the supercomputer but leads to an increase in computing time. Here, we observe that a splitting-simulation S20 require 19.2% more computing time than the reference simulation const. N_P87. If applied, merging allows a massive reduction of the number of superdroplets, reducing the computing time by 18% and the storage demand (which is proportional to the number of superdroplets) by at least by 7% compared to simulations applying only splitting (Fig.13a). All in all, the simulation applying both splitting and merging, is only 1.2% slower than the reference simulation const. N_P 87.

• **page 15 line 13:** The work by Dziekan and Pawlowska (2017) shows that when used in high-enough resolution the lagrangian methods truly do resolve the collisions between droplets. The tests presented in Unterstrasser et al. (2017) also suggest that when initialized correctly and when using a good algorithm for representing collisions the lagrangian microphysics schemes can represent collisions for coarser resolution settings (i.e low initial super-droplet concentration). The splitting and merging algorithm presented here is a valid improvement. It is especially important for large eddy simulation applications when by

necessity the lagrangian schemes have to be used with low super-droplet concentrations. Nevertheless in my opinion, saying that in general the lagrangian methods are known to insufficiently represent collisions is not justified.
Author's answer: Sorry for this misunderstanding. This statement is based on the insufficient representation of the collision growth of LCMs under certain initializations when a constant and large weighting factor is used. We definitely agree that LCMs with different initialization methods are able to represent collision very well (e.g. in box models) even without splitting. However, in certain applications it is not always possible to use such initialization methods (like singleSIP or multiSIP).
Modification (page 16 line 12): These models are able to represent collision and coalescence well (Unterstrasser et al., 2017;Dziekan and Pawlowska, 2017). Under certain conditions, however, they are known to insufficiently represented this process.
These conditions occur when the number of superdroplets is low and, accordingly, the number of real droplets represented by each superdroplet (the so-called weighting factor) is high, leading to an oversimplified representation of the droplet size distribution (DSD) (Riechelmann et al., 2012; Unterstrasser et al., 2017).

3 Minor comments

• The Lagrangian particles used to represent droplets are named differently by different modeling groups: super-droplets, simulation particles, etc. The original term super-droplet was introduced by Shima et al. (2009). Instead of using another notation superdroplet it would be better to follow the notation that is already used by others.
Author's answer: This was our attempt to establish the word, after consultation with native English speakers, in its the most correct variant.

• **page 1 line 16:** Are the references meant to be chronologically or alphabetically ordered?
Author's answer: In the revised version they are chronologically ordered.
Modification (page 1 line 16): (Shima et al., 2009; Sölch and Kärcher, 2010; Andrejczuk et al., 2010; Riechelmann et al., 2012; Arabas et al., 2015; Naumann and Seifert, 2015; Grabowski et al., 2018; Sardina et al., 2018)

• **page 1 line 16:** A couple more references to lagrangian microphysics applications: Lee et al. (2014), Arabas et al. (2015), Sardina et al. (2018)

Author's answer: Arabas et al. (2015) and Sardina et al. (2018) added in revised version. In our mind the citation of Lee et al. is not a useful citation.
Modification (page 1 line 16): (Shima et al., 2009; Sölch and Kärcher, 2010; Andrejczuk et al., 2010; Riechelmann et al., 2012; Arabas et al., 2015; Naumann and Seifert, 2015; Grabowski et al., 2018; Sardina et al., 2018)

• **page 1 line 23**: Which of the previously cited works use all-or-nothing algorithm?
Author's answer: The basic idea of the all-or-nothing algorithm is based on Shima et al. (2009) and Sölch and Kärcher (2010). Moreover this approach is used in the works of Arabas et al. (2015), Dziekan and Pawlowska (2017), and Hoffmann et al. (2017).
Modification (page 1 line 24): (based on Shima et al. (2009) and Sölch and Kärcher (2010), and used by Arabas et al. (2015), Dziekan and Pawlowska (2017), and Hoffmann et al. (2017)) exhibits the best performance, i.e., it agrees well with analytical solutions or other modeling approaches used to represent collection. Using an unfortunate initialization of superdroplets with equal weighting factors, however, even the all-or-nothing algorithm struggles to represent the precipitation process correctly

• **page 2 line 3**: What is a large weighting factor and a large number of super-droplets? Could you provide an order of magnitude estimate of those for a typical large eddy simulation grid box?
Author's answer: A large weighting factor is in the magnitude of 10^9. Typical LES applications with a grid size in the order of 10m and a typical super-droplet concentration of 100 per grid box need such weighting factors to represent number concentrations of 100 cm^{-3}. Even though the weighting factor changes due to collision and coalescence the reduction is insufficient for large droplets (r>100µm) to represent rain droplets statistically appropriate. Consequently, it is essential to have a large amount (in the magnitude of 10-100 per grid-box) of superdroplets representing large droplets with small weighting factors.
Modification (page 2 line 6): [..](with accordingly large weighting factors, approximately 10^9 for typical LES-LCM applications)[..].
[..](in the magnitude of 10-100 per grid-box with accordingly small weighting factors) [..].

• **page 2 line 30:** Is it more correct to say that it is a probability that super droplet m will collect super droplet n?
Author's answer: No, since the number of superdroplets does not change due to collisions and coalescence.

• **page 2 line 30:** An alternative is to consider for collisions only the non-overlapping pairs and

scale the probability - see section 5.1.3 in Shima et al. (2009) or section 5.1.4 in Arabas et al. (2015). This allows for the collision algorithm to scale linearly and not quadratically with the number of super-droplets. Maybe it should be mentioned?
Author's answer: In our opinion, this is a too detailed discussion and out of focus of the manuscript.

• **page 6 line 14:** Are the super-droplets sorted with regard to their size in memory? Or in other words are the super-droplets merged with the most similar super-droplet in a given grid-box?
Author's answer: No, super-droplets are sorted with regard to their position in a given grid-box. This is due to an optimized method for the interpolation of velocities to particle positions (see Marong et al. 2015). Nevertheless, since only particles with radii smaller than 0.1µm are merged in this study, the effects can can be neglected. If explicit activation is considered merging should be modified.
Modification (page 6 line 19): Moreover, a more advanced method was tested, in which the most similar droplets (within one grid box) concerning their mass are merged.
These simulations show no different results. However, due to sorting processes the computing time is increased in comparison to the simple method.

• **page 6 line 26:** Is diffusional growth allowed in the box model simulations? If yes, what is the assumed saturation? It is confusing with regard to line 15 on page 12. - Saying that collisions dominate the droplet growth in the box simulations suggests that there are other processes considered.
Author's answer: No, diffusional growth is not allowed in the box-model simulations. We think there must be a misunderstanding: Page 12 line 15 refers to the single cloud setup (not the single box setup), where we are simulating an idealized shallow cumulus cloud in form of a rising warm air bubble. In that case diffusional growth is considered as well as collisional growth and all (thermo-)dynamics.
Modification (page 6 line 30): Therefore, the box model simulation consider collection as the only microphysical process.

• **page 6 line 30 (and onward):** It's a bit confusing to talk about grid boxes when using a single box model setup. There is no real computational grid here.
Author's answer: We agree for the single-box method. However, for the multi-box approach grid properties cannot be neglected. Talking about grid boxes is valid for consistency reasons.
Modification (page 7 line 2): Although zero-dimensional simulations do not have a spatial extent, allocating a certain weighting factor requires a reference volume to represent a defined

droplet concentration.

• **page 6 line 30:** Where does the assumption that the box dimensions are $\Delta x = \Delta y = \Delta z = 20$m matter for the lagrangian scheme? Is it enough to say that the box volume is 8∗10^3m3?
Author's answer: We partially agree to this comment.
Modification (page 7 line 3): Therefore, the volume of a grid box is $8 \cdot 10^3$ m^3 , which corresponds to an isotropically spaced grid with $\Delta x = \Delta y = \Delta z = 20$ m.

• **page 7 line 1:** How many boxes are used? How are the boxes in multi-box approach located with regard to each other? What are the boundary conditions?
Author's answer: In the single-box approach, an ensemble of 25,344 grid-boxes is simulated. For the Multi-Box approach also 25,344 grid-boxes are used. However, they a horizontal exchange of super-droplets due to sub-grid scale velocities is allowed. Lateral boundary conditions are cyclic.
Modification (page 7 line 8): In contrast to the calculation of in- dependent grid boxes, the multi-box approach allows superdroplets to move from one grid box to the next by prescribing a stochastic velocity (but no mean motion) in (7), using 25,344 grid boxes, as in the single-box ensemble above, with cyclic boundary conditions among which the superdroplets are allowed to move.

• **page 7 line 6:** As stated in my first major comment - I don't agree that the initialization with constant weighting factors is a standard. Because it is such a bad initialization for representing collisions the new splitting algorithm should also be tested with a better initialization.
Author's answer: In the reviewed version we show some box-simulation results with a different initialization. However, the method of choice for "real cloud" applications is to start with an a certain superdroplet concentration and a constant weighting factor since it is unknown which particles will grow the most. Initializing the superdroplets with randomly chosen weighting factors or with weighting factors considering a prescribed aerosol spectrum also do not solve the problem, that large droplets are represented with unrealistic high weighting factors.
Therefore, we think our work provides useful information for the community.
Some examples for using constant weighting-factor in LCM applications are added as citations.
Modification (**page 7 line 15):** (e.g. Shima et al., 2009; Riechelmann et al., 2012; Naumann and Seifert, 2015, Hoffmann et al., 2017; Sardina et al., 2018)

• **Figure 2b:** Why is the LCM1000 behaves like a step function after 2500s?
Author's answer: The second moment is very sensitive to large radii of super-droplets. Collisions are discontinuous events and can produce significantly large droplets from one time-step to the next one.

• **Figure 3:** The plotting colors and patterns should be kept the same between Figs. 3,and 7 to allow easier comparison.
Author's answer: We agree.
Modification (Figure 5): Fig. 5 is changed.

• **page 10 line 25:** Is the initial super-droplet concentration again 87 per box?
Author's answer: Yes, it is!
Modification (page 11 line 20): Furthermore, all simulation are initialized identical with N_{init}= 87 superdroplets per grid box.

• **Figure 13a and 15c:** The notation N_{SIP} was never used before. The authors choose to refer to the lagrangian particles as super-droplets and not simulation particles.
Author's answer: Thanks, corrected in the reviewed revision!
Modification (Figure 13a and 15c): Changed axes in reviewed version to N_p.

• **page 14 line 15:** When it is not possible? What happens then?
Author's answer: Removed in revised version. This phrase was aimed at superdroplet specific quantities (such as initial number of super-droplets/to actual number of superdroplets), which were obviously not calculated in vanZanten et al (2011).
Modification (page 15 line 15): Moreover, the calculation of the domain-averaged quantities follows ~~(if possible)~~ the descriptions given in the original case.

• **page 16 line 24:** Dziekan and Pawlowska (2017) would be a valid reference here.
Author's answer: We agree and it is added in the reviewed revision.
Modification (15 line 24): (Shima et al., 2009; Riechelmann et al., 2012; Unterstrasser et al., 2017; Dziekan and Pawlowska, 2017)

• **page 15 line 27:** Figure 10 suggests that the maximum number of super-droplets $N_{P,max}$ is as important as the splitting radius r_{spl}?
Author's answer: That could be the case if the initialized number of super-droplets is not taken into account. Here, 87 particles per grid-box are used initially. Therefore, it can be concluded that it is important that the threshold $N_{P,max}$ is not to close to the initial value.

However, this also indicates that, if N_{init} is large enough, it does not change the results.
Modification (page 11 line 24): Since the initial superdroplet concentration is N_{init}= 87 for all configurations of $N_{P,max}$, it can be concluded that $N_{P,max}$ is a necessary but not crucial parameter as long as $N_{P,max} \geq 150$.

• **page 16 line 13:** The code of the Large Eddy Simulation model along with the new splitting and merging algorithm is available online and therefore fulfills the GMD requirements. It would have been great if the simple box model tests were available as a stand alone and easy to download and compile project. It would enable easy testing of the algorithm by others, for example this reviewer. It is by far too much coding to ask to do this now. I would just like to leave this comment as an idea for future development and testing.
Author's answer: Thanks for this comment. For future work we will heed this and will offer also our analysis tools and test cases which were developed and provide them in an own branch.

Improving Collisional Growth in Lagrangian Cloud Models: Development and Verification of a New Splitting Algorithm

Johannes Schwenkel[1], Fabian Hoffmann[1,*], and Siegfried Raasch[1]

[1]Institute of Meteorology and Climatology, Leibniz Universität Hannover, Hannover, Germany
*Current affiliation: Cooperative Institute for Research in Environmental Sciences (CIRES), University of Colorado, Boulder, Colorado, USA; NOAA Earth System Research Laboratory (ESRL) Chemical Sciences Division, Boulder, Colorado, USA

Correspondence: Johannes Schwenkel (schwenkel@muk.uni-hannover.de)

Abstract. Lagrangian cloud models (LCMs) are used increasingly in the cloud physics community. They not only enable a very detailed representation of cloud microphysics but also lack numerical errors typical for most other models. However, insufficient statistics, caused by an inadequate number of Lagrangian particles to represent cloud microphysical processes, can limit the applicability and validity of this approach. This study presents the first use of a splitting and merging algorithm designed to improve the warm cloud precipitation process by deliberately increasing or decreasing the number of Lagrangian particles under appropriate conditions. This new approach and the details of how splitting is executed are evaluated in box and single-cloud simulations, as well as a shallow cumulus test case. The results indicate that splitting is essential for a proper representation of the precipitation process. Moreover, the details of the splitting method (i.e., identifying the appropriate conditions) become insignificant for larger model domains as long as a sufficiently large number of Lagrangian particles is produced by the algorithm. The accompanying merging algorithm is essential to constrict the number of Lagrangian particles in order to maintain the computational performance of the model. Overall, splitting and merging did not affect the life cycle and domain-averaged macroscopic properties of the simulated clouds. This new approach is a useful addition to all LCMs since it is able to significantly increase the number of Lagrangian particles in appropriate regions of the clouds, while maintaining a computationally feasible total number of Lagrangian particles in the entire model domain.

1 Introduction

Lagrangian cloud models (LCMs) are a recently developed approach to simulate cloud microphysics (Shima et al., 2009; Sölch and Kärcher, 2010; Andrejczuk et al., 2010; Riechelmann et al., 2012; Arabas et al., 2015; Naumann and Seifert, 2015; Grabowski et al., 2018; Sardina et al., 2018). These models represent microphysics by individually simulated particles, so-called superdroplets, each representing a certain number of identical real droplets. This number is called multiplicity or weighting factor. These models have been used successfully to investigate various aspects of aerosol-cloud interactions (e.g., Andrejczuk et al., 2010; Hoffmann et al., 2015; Hoffmann, 2017) or precipitation processes (e.g., Naumann and Seifert, 2016; Hoffmann et al., 2017; Dziekan and Pawlowska, 2017).

Unterstrasser et al. (2017) have reviewed all three currently available LCM approaches for representing collection, from which the so-called all-or-nothing algorithm (based on Shima et al. (2009) and Sölch and Kärcher (2010), and used by Arabas

et al. (2015), Dziekan and Pawlowska (2017), and Hoffmann et al. (2017)) exhibits the best performance, i.e., it agrees well with analytical solutions or other modeling approaches used to represent collection. Using an unfortunate initialization of superdroplets with equal weighting factors, however, even the all-or-nothing algorithm struggles to represent the precipitation process correctly. The reason for that is easily explained. Cloud droplets cover a wide range of radii from micrometers to centimeters and a similarly wide range of abundances across this spectrum (e.g., Rogers and Yau, 1989). This system cannot be simplified to a couple of superdroplets (with accordingly large weighting factors, approximately 10^9 for typical LES-LCM applications). In fact, a large number of superdroplets (in the magnitude of 10 – 100 per grid box with accordingly small weighting factors) is needed to represent this range adequately. Since this is usually not the case, a few of the largest superdroplets may contain unrealistically the majority of all liquid water. In order to improve the statistics of these particles, Unterstrasser et al. (2017) suggested that the splitting of these particles can help to improve the representation of the precipitation process as it is already done for other microphysical processes (e.g., nucleation in ice clouds; Unterstrasser and Sölch, 2014).

The present study introduces and verifies a splitting algorithm designed to improve the precipitation process. Additionally, an accompanying merging algorithm is proposed that is able to unite superdroplets that are not required for an adequate representation of the precipitation process. Thus, the merging algorithm is essential to improve the computational performance of the LCM. Both algorithms are tested in zero-dimensional box-simulations, a three-dimensional simulation of a single cumulus cloud, and an established shallow cumulus test case. This paper is structured as follows. The next section briefly summarizes the used collection algorithm and the basic framework of the applied LCM. Section 3 introduces the splitting and merging algorithms, and section 4 shows results in which splitting and merging are applied. Finally, section 5 concludes the paper.

2 Basic Equations of the LCM

This sections gives a short overview on the LCM's basic equations. The applied LCM was initially developed by Riechelmann et al. (2012) and its current version is documented in Hoffmann et al. (2017). Besides collection, the LCM calculates diffusional growth as well as the transport of the superdroplets. These processes are coupled to the large-eddy simulation (LES) model PALM (Maronga et al., 2015), which solves the non-hydrostatic incompressible Boussinesq-approximated Navier-Stokes equations, and prognostic equations for the water vapor mixing ratio and potential temperature. In addition to these coupled simulations, we use a zero-dimensional box model, in which collision and coalescence is considered as the only microphysical process.

In the following, the applied collection algorithm will be summarized to show how collection affects a superdroplet's weighting factor, and to understand how collection and splitting interact. The reader is referred to Unterstrasser et al. (2017) for a more rigorous description of this all-or-nothing approach and to comparisons with other LCM collection algorithms. For the following, it is assumed that all superdroplets are sorted by their weighting factor such that $A_n > A_{n+1}$ (the case of $A_n = A_{n+1}$ will be discussed further below). For all superdroplet combinations with $1 \leq n < m \leq N_p$, where N_p is the number of superdroplets located in a grid box, the probability that one droplet of superdroplet m collects an arbitrary droplet of superdroplet n is given

by

$$p_{mn} = K(r_m, r_n)\frac{\Delta t}{\Delta V} \cdot A_n, \tag{1}$$

where Δt is the length of the collection time step, ΔV the volume of the grid box, r_n the radius of a droplet represented by superdroplet n, and K is the collection kernel (based on Hall (1980) for this study). Since p_{mn} is usually smaller than one, collections only occur if $p_{mn} > \xi$, where ξ is a random number uniformly chosen from the interval $[0, 1]$. This probabilistic approach ensures that the number of collections calculated in the model is identical to the number of collections resulting from Eq. (1) if averaged over a sufficiently long period of time.

If a collection takes place, each droplet of superdroplet m will collect one droplet of superdroplet n. This results in commensurate changes in the weighting factor A_n and the individual droplet mass $m_m = A_m \cdot 4/3\pi\rho_l r_m^3$ with the liquid water density ρ_l, while A_m and m_n remain unchanged:

$$\widehat{A}_m = A_m \qquad \text{and} \qquad \widehat{A}_n = A_n - A_m, \tag{2}$$

$$\widehat{m}_m = m_m + m_n \qquad \text{and} \qquad \widehat{m}_n = m_n, \tag{3}$$

where $\widehat{(..)}$ marks the variable after collection.

If $A_m = A_n$, the above-described collection would result in one superdroplet with a zero weighting factor. To avoid deleting this superdroplet, the droplets of the superdroplet that has grown by collection are distributed equally among the involved superdroplets m and n:

$$\widehat{A}_m = \widehat{A}_n = A_m \,/\, 2, \tag{4}$$

$$\widehat{m}_m = \widehat{m}_n = 2\, m_m. \tag{5}$$

Diffusional growth is described by

$$r_n \frac{dr_n}{dt} = \frac{S}{F_k + F_d} f(r_n). \tag{6}$$

The ventilation effect $f(r_n)$ describes the accelerated evaporation of large drops. S is the supersaturation (calculated in the LES), and F_k and F_d are coefficients considering the effects of heat conduction and the diffusion of water vapor, respectively (see, e.g., Rogers and Yau, 1989). Note that curvature and aerosol solute effects as well as gas-kinetic effects are neglected in (6), but this equation is appropriate for the purpose of this study which focuses on the precipitation process, i.e., larger droplets for which these processes are irrelevant.

Transport of each superdroplet is described by

$$\frac{dX_n}{dt} = u(X_n) + \widetilde{u}_n, \tag{7}$$

where X_n is the location of the superdroplet, u the LES resolved velocity interpolated to the superdroplet's location, and $\widetilde{u}$ is a stochastic velocity component to parameterize subgrid-scale fluctuations not resolved in the LES (see, e.g., Sölch and Kärcher, 2010).

3 Splitting and Merging

The following subsections will introduce techniques for the interactive modification of the number of superdroplets by splitting and merging. This is ~~fundamentally~~ different from most previous LCM approaches, in which the number of superdroplets is set in the beginning of the simulation and remains constant thereafter (unless precipitation scavenges superdroplets). Note that the splitting and merging algorithms will be tested for the all-or-nothing collection approach, but they are similarly applicable to the average-impact approach introduced by Riechelmann et al. (2012).

3.1 Splitting

Splitting takes place if a superdroplet fulfills certain criteria. First, the radius of the superdroplet needs to be greater than or equal to a threshold r_{spl}. This is necessary to limit splitting to the region of interest, i.e., coalescing droplets for which an improved statistical representation is required. Second, the weighting factor of the superdroplet needs to be greater than or equal to a threshold A_{spl} to avoid excessive and potentially useless splitting. And finally, A_{spl} is required to be at least larger than η_{spl}, which is the number of superdroplets in which the superdroplet is split. This ensures that no superdroplets with an unrealistic weighting factor of less than 1 are created.

The numerical implementation of the splitting can be understood as cloning of the superdroplet that has been determined to be split. In addition to the already existing superdroplet, $\eta_{\text{spl}} - 1$ new superdroplets are created. To conserve the total amount of represented droplets, the weighting factor of these η_{spl} superdroplets is reduced to

$$A_n^* = \frac{A_n}{\eta_{\text{spl}}}. \tag{8}$$

Note that all η_{spl} superdroplets have identical properties immediately after splitting, including their location. However, each superdroplet will develop an individual trajectory independent from the others due to the stochastic velocity component in (7), which is determined individually for each superdroplet.

In a first straightforward approach, the thresholds r_{spl}, A_{spl}, and the splitting factor η_{spl} are explicitly prescribed. In the following this method is abbreviated as S-mode, where the S stands for simple.

In a more advanced method (abbreviated *G*, standing for gamma distribution), the threshold A_{spl} and the splitting factor η_{spl} are estimated from an idealized gamma distribution, which is assumed to describe the distribution of droplets larger than r_{spl} in each grid box of the simulated model domain (e.g., Ulbrich, 1983):

$$n(r) = N_0 r^{\mu} \exp(-\lambda r), \tag{9}$$

where $n(r) \cdot \mathrm{d}r$ states the number of particles per unit volume in the size range $(r, r + \mathrm{d}r)$. Here, N_0 is the intercept, μ is the shape, and λ is the slope parameter of the gamma distribution. These parameters are calculated as

$$N_0 = \frac{N_r}{\Gamma(\mu+1)} \lambda^{\mu+1}, \tag{10}$$

$$\lambda = \left[\frac{\pi \rho_{\text{l}}}{6} (\mu+3)(\mu+2)(\mu+1) \overline{\text{x}_{\text{r}}}^{-1} \right]^{\frac{1}{3}}, \tag{11}$$

and

$$\mu = \frac{(1-\zeta)n+1}{\zeta-1}, \tag{12}$$

where N_r is the number concentration of droplets with $r \geq r_{\text{spl}}$, Γ is the gamma function, ρ_{l} is the density of liquid water, $\overline{\text{x}_\text{r}}$ is the mean geometric radius, and ζ is a factor calculated as

$$\zeta = \frac{M_0 M_2}{M_1^2}, \tag{13}$$

where M_k is the k-th moment of the mass density distribution (see Seifert, 2008). The calculation of these moments in the LCM framework will be described in section 4.1.1.

The assumed drop size distribution (DSD) is calculated from $n_{\text{bin}} = 100$ logarithmically spaced bins. (Larger values for n_{bin} did not alter the results.) The center of bin i is calculated as

$$r_{\text{bc},i} = 10^{\log_{10}(r_{\text{min}})+i\nu}, \tag{14}$$

where

$$\nu = \frac{\log_{10}(r_{\text{max}}) - \log_{10}(r_{\text{min}})}{n_{\text{bin}} - 1}. \tag{15}$$

The minimum and maximum radius of the discretized spectra are denoted with r_{min} and r_{max}, respectively. Here, these values are set to $r_{\text{min}} = r_{\text{spl}}$ and $r_{\text{max}} = 5\,\text{mm}$, which ensures that the whole spectrum of droplet sizes is included. Furthermore, the boundaries of bin i are given by $r_{\text{bb},i} = 10^{\log_{10}(r_{\text{min}})+(i-0.5)\cdot\nu}$ and $r_{\text{bb},i+1}$. Hence, the width of bin i is $\Delta r_i = r_{\text{bb},i+1} - r_{\text{bb},i}$.

It is assumed that the weighting factor of a superdroplet should be smaller than or equal to the approximated number of droplets in the corresponding bin of the discretized gamma distribution. Thus, the weighting factor threshold is determined by

$$A_{\text{spl},i} = \max\left[n_i(r_{\text{bc},i}) \cdot \Delta r_i \cdot \Delta V,\ 1\right]. \tag{16}$$

Accordingly, the number of newly generated superdroplets depends on the ratio of the initial weighting factor to the estimated number of droplets using the gamma distribution:

$$\eta_{\text{spl}} = \left\lfloor \frac{A_n}{A_{\text{spl},i}} \right\rfloor. \tag{17}$$

Since only a positive integer of superdroplets can be generated, the splitting factor is rounded down to the nearest whole number.

No matter which splitting mode is chosen, the splitting operations are executed at each time step of the LCM. Due to limited computational resources, the generation of new superdroplets must be restricted to a feasible amount. Hence, two limitations are introduced. The first restriction is the maximum splitting factor η_{max}, i.e., the maximum number of clones produced per splitting. This parameter is used for the G-mode, in which (17) might not be well-defined in the case of large droplets for which $A_{\text{spl},i}$ approaches zero. The second limitation ensures a computationally feasible number of superdroplets in every grid box by introducing a fixed maximum $N_{\text{P,max}}$. Accordingly, splitting operations are only executed if the number of superdroplets in one grid box is smaller than $N_{\text{P,max}}$. The latter threshold is applied for the G- and the S-mode. A suitable choice of these limits will be presented in section 4.1.2.

3.2 Merging

As a consequence of the potentially massive generation of new superdroplets due to splitting, the total number of superdroplets may increase sharply, which makes simulations computationally very expensive. For this reason, a merging algorithm was developed to decrease the number of superdroplets in order to reduce the required computational resources.

To avoid an impact of merging on micro- or macrophysical properties of the cloud, the algorithm is only executed in non-cloudy grid boxes (liquid water is lower than $q_l < 0.01\,\mathrm{g\,kg^{-1}}$). Accordingly, cloudy regions, in which a high number of superdroplets is necessary for the correct representation of potential collisional growth, are left unaffected. Furthermore, it is required that the merged superdroplets are smaller or equal to $r_{\mathrm{mer}} = 0.1\,\mu\mathrm{m}$, which ensures that only evaporated superdroplets are affected, and not raindrops that precipitate from the cloud. Additionally, merging is only executed in grid boxes in which the initial superdroplet concentration is exceeded and superdroplets exhibit a weighting factor that is smaller than a certain threshold A_{mer}, rationally chosen to be smaller or equal to the initial weighting factor. This is done to avoid decreasing the LCM's baseline capability to represent DSDs set during initialization.

The algorithm is designed as follows. Based on the thresholds r_{mer} and A_{mer}, each superdroplet with $r_m \leq r_{\mathrm{mer}}$ and $A_m \leq A_{\mathrm{mer}}$ in a non-cloudy grid box is merged with the next superdroplet of the same grid box. Here, the next superdroplet is the superdroplet located next in the memory, which enables an efficient execution of the merging algorithm. The new weighting factor of the remaining superdroplet (index n) is mass-weighted and given by $A_{\mathrm{n}}^* = A_{\mathrm{n}} + A_{\mathrm{m}} \cdot r_{\mathrm{m}}^3 / r_{\mathrm{n}}^3$, while the other superdroplet (index m) is deleted. Accordingly, this leads to a new integral mass $M_n^* = M_n + M_m$, guaranteeing mass conservation. An averaging of other superdroplet properties (e.g., velocities components, radius, and location) is not implemented and probably not necessary for the correct representation of the cloud since merging is restricted to a cloud-free environment. Moreover, a more advanced method was tested, in which the most similar droplets (within one grid box) concerning their mass are merged. These simulations show no different results. However, due to sorting processes the computing time is increased in comparison to the simple method.

The use of the merging algorithm inside certain regions of the cloud where collection plays only a subordinate role is also conceivable. However, the (probably sophisticated) determination of necessary thresholds is not within the scope of this study. Furthermore, it must be mentioned that the merging algorithm does not conserve size and chemical composition of the aerosol. Therefore, for studies that explicitly consider aerosols, the merging algorithm needs to be adapted.

4 Applications

4.1 Box Model Simulations

In the following box simulations, the sensitivity of the LCM collection process to the number of simulated superdroplets, different splitting approaches, and the approaches' specific parameters is investigated. Therefore, the box model simulation consider collection as the only microphysical process.

4.1.1 Setup

Although zero-dimensional simulations do not have a spatial extent, allocating a certain weighting factor requires a reference volume to represent a defined droplet concentration. Therefore, the volume of a grid box is $8 \cdot 10^3\,\mathrm{m}^3$, which corresponds to an isotropically spaced grid with $\Delta x = \Delta y = \Delta z = 20\,\mathrm{m}$. The simulation time is $3600\,\mathrm{s}$ with a constant time step of $1\,\mathrm{s}$. To ensure adequate statistics, 25,344 boxes are calculated, and results are averaged over this ensemble. (The number of ensemble members represents the maximum amount of grid boxes which can be calculated on 4 computing nodes in an appropriate time.) In the following this method is referred as single-box model.

Besides the traditional single-box approach a new multi-box approach is introduced. In contrast to the calculation of independent grid boxes, the multi-box approach allows superdroplets to move from one grid box to the next by prescribing a stochastic velocity (but no mean motion) in (7), using 25,344 grid boxes, as in the single-box ensemble above, with cyclic boundary conditions among which the superdroplets are allowed to move. The stochastic velocity component is chosen is such a way that it corresponds to a kinetic energy dissipation rate of $\epsilon_{\mathrm{box}} = 0.01\,\mathrm{m}^2\mathrm{s}^{-3}$, which is typical for shallow cumulus clouds (e.g., Shaw et al., 1998).

This multi-box approach has one distinct advantage over the ensemble mean of the same amount of individual box model simulations (single-box model), which results from the difficulties to initialize a DSD with superdroplets of a constant weighting factor, as it is done in many applications of LCMs in the literature (e.g. Shima et al., 2009; Riechelmann et al., 2012; Naumann and Seifert, 2015; Hoffmann et al., 2017; Sardina et al., 2018). A single box model simulation suffers crucially from this initialization method due to a wrong representation of the largest and rarest superdroplets (Unterstrasser et al., 2017, their Fig. 17). In doing so, the rarest and largest, and therefore most important superdroplets for the collection process, are a priori over- or underestimated. An exchange of superdroplets between the collection boxes helps to mitigate this problem. Moreover, this new approach is closer to the representation of collection in three-dimensional simulations, in which a superdroplet is not bound to a single grid box.

The impact of different numbers of superdroplets per grid box and the use of splitting for the traditional single-box approach will be discussed first; then, the new introduced multi-box approach will be presented for both splitting and non-splitting cases. Box model simulations will be compared to the results of Wang et al. (2007), who used a high-resolution bin model. The purpose of this study is, however, not the exact reproduction of these results but a computationally efficient approximation to them using splitting. Accordingly, the initialization of the box simulation follows Wang et al. (2007), using an exponential initial DSD:

$$n(r, t = t_0) = \frac{3N_{\mathrm{init}}}{r_0^3} \cdot r^2 \exp\left(-\frac{r^3}{r_0^3}\right), \tag{18}$$

where $N_{\mathrm{init}} = 300\,\mathrm{cm}^{-3}$ is the droplet number concentration. The initial mean radius is $r_0 = 9.3\,\mu\mathrm{m}$, which leads to a liquid water content of $L_0 = 1\,\mathrm{g\,m}^{-3}$. Following Wang et al. (2007), we set the minimum droplet radius to $r_{\mathrm{min}} = 1.5\,\mu\mathrm{m}$. Superdroplet radii are then selected by a random generator which follows the distribution given by (18). All superdroplets receive

the same initial weighting factor:

$$A_{\text{init}} = \frac{N_{\text{init}} \cdot \Delta V}{N_{\text{P}}}, \tag{19}$$

which ensures the number concentration of $300\,\text{cm}^{-3}$. This method is also described as ν_{const}-init in Unterstrasser et al. (2017), which has been chosen in this study to resemble the initialization of superdroplets in less-idealized applications but also significantly hinders collisional growth.

As reference, the singleSIP initialization of Unterstrasser et al. (2017) is used for the single-box model, too. In contrast to the previously described initialization, the initial DSD is discretized using logarithmically spaced bins. The number of bins corresponds to the number of superdroplets. To each bin, a superdroplet with a corresponding mean radius and weighting factor is assigned. The maximum radius of the initial distribution is approximately $33\,\mu\text{m}$, which corresponds to a number of concentrations of $1/\Delta V$. This avoids superdroplets with a weighting factor less than 1. Note that this (not always applicable) initialization technique represents the inherent variability of droplet radii and their abundance across the initial spectrum much more accurately than the previously described method, and, therefore results in a much better agreement with literature references.

In addition to analyzing the DSD directly, the temporal development of the zeroth and second moment of the mass density distributions is examined. Due to mass conservation in all applied approaches, the first moment is constant in time and will not be shown. The moments of the mass distribution f_m are defined as

$$M_k = \int m^k f_m(m)\, \mathrm{d}m, \tag{20}$$

where m is the mass and $f_m(m)$ denotes the number concentration distribution. Note that the zeroth moment M_0 is the number concentration and the second moment M_2 is proportionate to the radar reflectivity, and thus highly sensitive to the largest droplets in the DSD.

For a given superdroplet ensemble the moments for each grid box are calculated with

$$M_k = \sum_{n=1}^{N_{\text{P}}} A_n m_n^k / \Delta V, \tag{21}$$

where m_n is the single droplet mass ($m_n = 4/3\pi\rho_l r_n^3$) of a superdroplet.

4.1.2 Box Model Results

First, the sensitivity of the collision algorithm to the number of superdroplets is examined using the LCM as a single-box model. Second, the improvements by the splitting method on collisional growth is evaluated. Subsequently, those investigations are repeated for the multi-box approach.

Single-Box Approach

Figures 1 and 2 show the mass density distribution after $3600\,\text{s}$ and the temporal development of the moments for the LCM applied as a single-box model using the singleSIP initialization by Unterstrasser et al. (2017). Each grid box is initialized with

a different number of superdroplets (colored lines). The reference solution of Wang et al. (2007) is shown as a black solid line. Figure 1 shows that even with 87 superdroplets the solution of Wang et al. (2007) can be reproduced well and a further increase in the number of superdroplets only leads to minor improvements. The small deviations between the bin model solution and the LCM can be traced back to the different solution of the collection equation (e.g., Dziekan and Pawlowska, 2017). Overall, it can be seen that the solution of the LCM converges with an increasing number of superdroplets. The moments of mass distribution (Fig. 2) also show convergence with an increasing number of superdroplets. This good representation of collision growth is in line with the results with Unterstrasser et al. (2017).

Now, Figs. 3 and 4 show the same quantities but for the initialization with identical weighting factors. In Fig. 3, a significant deviation of the mass density distribution of the reference solution can be seen for all configurations. An excessively pronounced first maximum is found for all superdroplet concentrations, while the second maximum is at too small droplet sizes. Also, fluctuations ~~oscillations~~ occur for radii larger than $100\,\mu\mathrm{m}$, resulting from insufficient superdroplet statistics in this range. However, as the initial number of superdroplets increases, the depletion of the first maximum and the development of the second maximum is reproduced better. Figure 4a shows that in all cases the decrease in the number concentration is underestimated. Also for the second moment (Fig. 4b), values are predicted too low in nearly all cases. All in all, it can be observed that an increase in the number of superdroplets leads to a better agreement of the results with the bin-model even though difference are still significant for 1000 superdroplets per grid box.

In Fig. 5 and 6 the mass density distribution after $3600\,\mathrm{s}$ and the temporal development of the moments applying the splitting algorithm in different configurations are shown. Again, the splitting modes are abbreviated with S for the simple splitting method and G for using the splitting method based on a gamma distribution. The number following S or G indicates the splitting radius in microns. For all simulations, the maximum permissible number of superdroplets per grid box is limited to $N_{\mathrm{P,max}} = 1000$. The maximum splitting factor is $\eta_{\mathrm{max}} = 20$. By selecting these limits, which are chosen to represent the upper limit of computationally feasible three-dimensional simulations, it is possible to obtain an estimate of the quality of the individual splitting methods. The influence of the choice of these parameters is discussed below. All simulations are initialized with $N_{\mathrm{P}} = 87$ superdroplets per grid box.

The black dashed line ($const.$) shows the reference LCM case in which no splitting is applied. Comparing the non-splitting case to splitting cases the results are significantly improved with respect to the reference solution. More precisely, the fluctuations ~~oscillations~~ that occur for large droplet radii are successfully removed by splitting. Furthermore, a better representation of the second maximum is achieved by splitting, too. Independent of the splitting mode, simulations with the same splitting radius provide similar results. The only exception is between the simulations *G10* and *S10*, in which the assumed gamma distribution enables effective splitting at slightly larger radii in $G10$ compared to *S10*. This results in a better agreement of *S10* with the bin reference. In general, a reduction of the splitting radius leads to an improved representation of the mass density distribution. However, for all splitting simulations the reduction of the first maximum is underestimated, while the second maximum is only inadequately represented.

Similar conclusions are possible from Fig. 6, in which the timeseries of zeroth and second moment of the DSD are shown. The best agreement for the number concentration is achieved by *S10*, where many superdroplets are cloned at a very early stage.

For all splitting configurations, the second moment shows a strong improvement in comparison to the LCM reference case without splitting (*const.*) where this value is largely underestimated. Accordingly, splitting leads to an improved representation of the collisional growth in LCMs but there are still very large deviations from the bin reference.

These results exhibit how strongly collisional growth suffers from the initialization with a constant weighting factor, consistent with Unterstrasser et al. (2017). Since large superdroplets are initialized only in a few grid boxes, collisional growth is subject to a great variability in the different realizations among the ensemble. Due to that, the following subsection will repeat this investigations using the multi-box approach, which reflects the collisional growth in 3D-applications more appropriately.

Multi-Box Approach

Figure 7 shows the mass density distribution after $3600\,\mathrm{s}$ time for different numbers of superdroplets (colored lines) using the multi-box approach without splitting. One can see that as the number of superdroplets increases, a better agreement with the bin model is achieved. Especially the simulations with 512 and 1000 superdroplets per grid box can reproduce the mass density distribution well. However, for these cases, a stronger decrease of the first maximum is observed. This can be attributed to accelerated accretion, which is favored by the combination of a few large droplets with an overestimated weighting factor and a large number of superdroplets with radii of about $10\,\mu\mathrm{m}$. In contrast, a decelerated depletion of the first maximum and a weaker second peak are detected for simulations with a lower number of superdroplets. This results from the insufficient representation of the initial DSD, especially that of large droplets, which are crucial for effective collisional growth.

In Fig. 8, the temporal evolution of the number concentration and the second moment are shown. In simulations with a high number of superdroplets, a too strong reduction of the number concentration is predicted, and contrary the decrease of the zeroth moment is underestimated in cases with only 15 and 37 superdroplets. This tendency is also observed for the second moment. Simulations with a high number of superdroplets overestimate the reference, whereas simulations with only a few superdroplets result in too low values. However, comparing the results of the non-splitting cases ($const.$) in the single-box and the multi-box simulations, the latter already provides improved results with respect to the bin model. The results show that this initialization artifact can be successfully mitigated by the newly introduced stochastic exchange between the grid boxes. For typical applications, however, the required amount of at least 512 superdroplets per grid box, necessary to derive satisfying results without splitting, is computationally unfeasible.

To maintain a reasonable amount of superdroplets, these box-simulations will be repeated now, using the splitting approach. Here, all parameters (initializing all simulations with 87 superdroplets per grid box) and splitting thresholds are identical as for the single-box approach described above but the superdroplets are now allowed to move between grid boxes.

Figure 9 shows the mass density distribution after $3600\,\mathrm{s}$ for different splitting configurations. Clear differences in the consistency with the bin reference solution can be seen. In particular, the simulations *S10* and *G10* show a good agreement with the results of Wang et al. (2007). In both cases, the bimodal shape of the spectrum is represented well. However, for the other simulations, the deviation from the reference solution increases with increasing splitting radius, but less with the splitting mode. Both simulations with a splitting radius of $40\,\mu\mathrm{m}$ show no improvements in comparison to a simulation without splitting (*const.*, black dashed line), except in the right tail of the distribution. Figure 10 shows the moments for the different splitting

configurations. The two plots indicate a slightly faster precipitation process than in the bin model, but the general agreement with the reference is much higher than without splitting (Fig. 8). Again, general differences between the bin model and the LCM are caused by the initialization, which cannot be fixed by splitting. The initialization with constant weighting factors will always deviate from the exponential initialization used by Wang et al. (2007). Therefore, subsequent collisions, which are improved by splitting, cannot agree with the bin-solution by Wang et al. (2007) whatsoever. In general, the decreasing difference among the different LCM simulations, as it is occurring due to splitting, needs to be seen as a proof of concept, and not the comparison with the bin results.

All in all, it is shown that collisional growth is better represented by using the splitting method in both the single-box and multi-box simulations. Furthermore, the choice of the splitting mode is secondary, but the splitting radius is identified as the most crucial parameter. The multi-box simulations exhibit a distinct advantage over the single-box simulations. Due to the presence or absence of sufficiently large droplets that might initiate collision and coalescence, as a result of the initialization, collisional growth can be be overestimated in certain grid boxes while it is underestimated in others. Splitting and the subsequent stochastic exchange are able to distribute these so-called precipitation embryos among the entire ensemble where they are able to initiate collision and coalescence as sketched in Fig. 11, which would not be possible in the single-box approach.

Sensitivity to Splitting Thresholds

The limiting parameters of the splitting algorithm are now examined in sensitivity studies using the multi-box approach. For this purpose, the parameters of the maximum possible number of superdroplets per grid box $N_{\mathrm{P,max}}$, the maximum splitting factor η_{max}, and the splitting radius r_{spl} are varied for the splitting mode *G*, which base state is defined as $r_{\mathrm{spl}} = 10\,\mu\mathrm{m}$, $\eta_{\mathrm{max}} = 20$, and $N_{\mathrm{P,max}} = 1000$. This base state is varied by individually changing the parameters r_{spl}, η_{max}, and $N_{\mathrm{P,max}}$. Furthermore, all simulation are initialized identical with N_{init}= 87 superdroplets per grid box.

Figure 12 a shows the mass density distributions after 3600 s for different values for $N_{\mathrm{P,max}}$. We find that a value of $N_{\mathrm{P,max}} = 150$ is sufficient to reach convergence for this setup. Since the initial superdroplet concentration is N_{init}= 87 for all configurations of $N_{\mathrm{P,max}}$, it can be concluded that $N_{\mathrm{P,max}}$ is a necessary but not crucial parameter as long as $N_{\mathrm{P,max}} \geqslant 150$. This reduction of the maximum number of superdroplets per grid box results in a reduction of the computational time by a factor of 15 compared to the simulation with $N_{\mathrm{P,max}} = 1000$.

The sensitivity studies for the maximum splitting factor show that this has no influence on the results (Fig. 12 b). An explanation for this is that the algorithm is executed at every time step and thus only the clone rate but not the absolute number of the clones is affected. More precisely, a low value of η_{max} may reduce how many clones are produced at a time step. However, results show that this effect is negligible since a superdroplet will be cloned sufficiently fast at the subsequent time steps as long as $N_{\mathrm{P}} \leq N_{\mathrm{P,max}}$.

As shown before, the development of the spectrum is highly sensitive to the choice of the splitting radius. Figure 12c shows that the results converge with decreasing splitting radius, with no significant deviations for configurations with $r_{\mathrm{spl}} \leq 15\,\mu\mathrm{m}$. This can be attributed to the fact that especially the largest droplets (in this case with radii of approximately $15\,\mu\mathrm{m}$) are

crucial for initiating the collisional growth. Accordingly, an improved representation of these droplets leads to an improved representation of the whole collisional growth process.

4.2 Single Cloud

4.2.1 Setup

In this case, we are simulating an idealized shallow cumulus cloud in form of a rising warm air bubble as in Hoffmann et al. (2017). The model domain is $1920\,\mathrm{m} \times 7680\,\mathrm{m} \times 3840\,\mathrm{m}$ in x-, y- and z-direction, respectively. An isotropic grid spacing of 20 m is used. The simulation time is 3000 s using a constant time step of $0.1\,\mathrm{s}$. The warm air bubble is triggered by a Gaussian-shaped potential temperature perturbation θ^*

$$\theta^*(y,z) = \theta_0 \cdot \exp\left[-\frac{1}{2} \cdot \left(\left(\frac{y-y_\mathrm{c}}{\sigma_\mathrm{y}}\right) + \left(\frac{z-z_\mathrm{c}}{\sigma_\mathrm{z}}\right)\right)\right], \tag{22}$$

where $\theta_0 = 0.4\,\mathrm{K}$ is the maximum temperature difference, which decreases with a standard deviation of $\sigma_\mathrm{y} = 200\,\mathrm{m}$ and $\sigma_\mathrm{z} = 150\,\mathrm{m}$ in y- and z-direction, respectively. The center of the bubble is set to $y_\mathrm{c} = 3840\,\mathrm{m}$ and $z_\mathrm{c} = 170\,\mathrm{m}$. Due to the two-dimensional character of the temperature excess, the initial temperature perturbation is elongated homogeneously along the x-axis.

The initial profiles for temperature and specific humidity are based on the shallow cumulus case by vanZanten et al. (2011). Note that no background winds, large-scale forcings, or surface fluxes are considered. The superdroplets are released at the beginning of the simulation and are uniformly distributed in the entire model domain. For all three directions in space, the average distance of the superdroplets is initially 4.5 m. This results in a superdroplet concentration of approximately 87 superdroplets per grid box and roughly $4.55 \cdot 10^8$ superdroplets in total. Using a weighting factor of $A_\mathrm{init} = 9.0 \cdot 10^9$, an initial cloud condensation nuclei (CCN) concentration of $100\,\mathrm{cm}^{-3}$ is represented. Additionally, simulations with 15 and 186 superdroplets per grid box are carried out, in which the weighting factor is adjusted such that the CCN concentration of $100\,\mathrm{cm}^{-3}$ is retained. If merging is applied, only superdroplets with a radius smaller than $r_\mathrm{mer} = 0.1\,\mu\mathrm{m}$ and with a weighting factor smaller than $A_\mathrm{mer} = A_\mathrm{init}/2$ are allowed to merge.

At the surface, superdroplets are absorbed if their radius is larger than $1.0\,\mu\mathrm{m}$. For smaller particles, a reflection boundary condition is assumed to avoid that the surface acts as a CCN sink. Horizontal boundaries are prescribed with cyclic conditions. Moreover, for collision and coalescence, the kernel by Hall (1980) is used. An overview of all conducted simulations is given in Table 1.

4.2.2 Single Cloud results

Microphysical Properties

Figure 13 shows the cloud averaged mass density distribution at $t = 1800\,\mathrm{s}$ for the configurations listed in Tab. 1. The left part of the spectrum is reproduced quantitatively consistent in all cases. This implies that both the splitting and the merging process have no artificial impact on the diffusional growth process, which prevails in this region of the spectrum. However, the right tail

Table 1. Summary of the main parameters for the single cloud simulations.

Simulation	N_P	initial weighting factor	Splitting	r_{spl}	$N_{P,max}$	$\eta_{spl/max}$	Merging
const. N_P15	15	5.0×10^{10}	no	-	-	-	no
const. N_P87	87	9.0×10^{9}	no	-	-	-	no
const. N_P186	186	4.3×10^{9}	no	-	-	-	no
S10	87	9.0×10^{9}	yes	10 µm	150	20	no
S20	87	9.0×10^{9}	yes	20 µm	150	20	no
S20 merging	87	9.0×10^{9}	yes	20 µm	150	20	yes
G20	87	9.0×10^{9}	yes	20 µm	150	20	no
G20 merging	87	9.0×10^{9}	yes	20 µm	150	20	yes

of the DSDs differs significantly when the splitting algorithm is applied. The biggest drops are almost 350 µm smaller for the reference case (black lines) compared to simulations with splitting. Furthermore, splitting effectively reduces the fluctuations which occur in the reference cases for radii above 100 µm. The mass density distributions imply that the choice of the splitting mode does not affect cloud microphysical results. Likewise, the simulation $S10$, in which the splitting radius is reduced to $r_{spl} = 10\,\mu m$, shows almost no difference in the mass density distribution compared to cases with $r_{spl} = 20\,\mu m$. Thus, it can be deduced that a splitting radius of $r_{spl} = 20\,\mu m$ is sufficient for this cloud. Further investigations (not shown) in which r_{spl} is successively increased to $30\,\mu m$ show that a larger splitting radius leads to strong deviations from simulations with smaller splitting radius. This indicates that droplets with radii larger than $20\,\mu m$ need to be represented in a statistically sufficient way to initiate the precipitation process correctly. It should be emphasized, however, that these results are only valid for a cloud with a relatively strong diffusional radius growth. A reduction of the splitting radius might be required for settings in which collisions dominate the droplet's growth at smaller radii as it is the case in the previously presented box-simulations.

This behavior can be ascribed to different requirements on the superdroplet number for the convergence of different growth processes. The left part of the spectrum is dominated by diffusional growth which can be sufficiently represented by just a couple of superdroplets per grid box. By contrast, collisional growth is highly sensitive to the superdroplet number and the correct representation of large droplets. An improved representation of these droplets is ensured by the splitting algorithm, no matter what splitting mode is used.

The improved statistics of large superdroplets are also shown in Fig. 14, where the absolute number of superdroplets per logarithmic radius ($\log(r)$) bin is presented. It is noticeable that in the reference simulations, this number decreases significantly for larger droplets (starting from a radius of approximately $r = 20\,\mu m$). In simulations in which no splitting operations are carried out, the largest droplets are represented by only a few tens of superdroplets in the whole model domain. For the S-mode, the superdroplet concentration is kept almost constant (except in the right tail) for all splitting cases. For the G-mode a second maximum at $100\,\mu m$ can be observed. This can be related to the calculation of the splitting criterion. The approximation

of the mass density distribution by a gamma distribution results in a somewhat lower splitting factor for superdroplets close to the splitting radius in comparison to the S-mode, which shifts the superdroplet production to larger radii in the G mode.

Macrophysical Properties

In Fig. 15, the development of the cloud is shown in timeseries of several macroscopic properties. The behavior of the different splitting configurations can be clearly seen in Fig. 15a, which depicts the ratio of the current superdroplet number to its initial value. In simulations without splitting, the superdroplet number remains nearly constant. A clear increase in the superdroplet number can be observed when splitting is used, with maximum increase of about 15 % for *S10*. In all other splitting cases, the increase in superdroplet number is notably lower and starts approximately 500 s later, which corresponds to the larger splitting radius of $r_{\text{spl}} = 20\,\mu\text{m}$. The lowest increase in superdroplet number is observed in the merging cases in which the maximum number of superdroplets is reached during the growing phase of the cloud and decreases in the dissipation stage.

Figure 15b and 15c show the temporal evolution of the liquid water path (LWP) and the rain water path (RWP). The RWP is defined as the integral mass of all droplets with $r \geq 40\,\mu\text{m}$. It is notable that the LWP is the same for all simulations, which emphasizes the mass conserving character of the splitting algorithm and its negligible impact on the general development of the cloud. ~~All splitting configurations show higher RWPs in comparison to the reference runs without splitting. This increase of up to 12% is a direct result of the improved collisional growth process in the splitting configurations, resulting in more numerous and larger rain drops. This is also observed for the radar reflectivity (Fig. 15d), which is proportional to the second moment of the DSD and hence more sensitive to larger droplets.~~ In the reference simulations (represented as a mean of 5 ensemble for each case) of Figs. 15c and 15d, one can seen an increase in the precipitation parameters (RWP, radar reflectivity and precipitation sum) for an increased number of superdroplets. However, the differences among the ensembles members are quite large,which is shown by the range (gray area) and the band of plus-minus one standard deviation from the mean (light blue area) derived from all 15 ensemble members. Overall, the splitting simulations have a slight tendency to compare better with the reference cases using 87 and 186 superdroplets. Admittedly, since the results are (for the most part) within one standard deviation, it can be concluded that splitting has no significant influence on the global precipitation parameters.

Figure 15e and 15f display the precipitation rate and the total precipitation reaching the ground. The precipitation rate in the reference simulations without splitting exhibit high temporal variances (black lines). Those variances are successfully reduced in all splitting simulations. This can be explained by the better representation of precipitation in the splitting simulations by a larger number of superdroplets, resulting in a more uniform removal of liquid water by precipitation. As expected from the RWP, splitting slightly increases the total precipitation.

Figure 16 shows the effect of splitting on the spatial distribution of rain after 2100 s simulated time for the $\text{N}_\text{P}87$ simulation (left panel) and the *S20* splitting simulation (right panel). Similar to the reduced temporal variance in the time series of the precipitation rate (Fig. 15e), the spatial variance is also significantly reduced using splitting. Again, the precipitation is represented by only few superdroplets in the simulation without splitting, which leads to very high, localized precipitation rates. Due to splitting, raindrops with large weighting factors are split into several superdroplets with smaller weighting factors, resulting in the more realistic spatial representation of the precipitation.

All in all, the splitting of large droplets, which results in an improved representation of the collision process and thus the DSD, also partly influences the macroscopic properties of the cloud. In particular, rain water content, radar reflectivity and precipitation rate are represented in a more realistic manner. Due to the improved statistics, the temporal and spatial variance of these parameters is significantly reduced. However, the whole cloud life-cycle, which is driven by the general dynamics and thermodynamics, is largely unaffected by splitting. Additionally, the merging shows no influence on the physical outcomes.

To estimate the increase in computing time due to splitting, we conducted three simulations (*const.* N_P87, *S20* and *S20 merging*) with comparable time measurements. Here, we observe that the splitting-simulation *S20* requires 19.2% more computing time than the reference simulation *const.* N_P87. If applied, merging allows a massive reduction of the number of superdroplets, reducing the computing time by 18% and the storage demand (which is proportional to the number of superdroplets) by at least by 7% compared to simulations applying only splitting (Fig. 15a). All in all, the simulation applying both splitting and merging, is only 1.2% slower than the reference simulation *const.* N_P87.

4.3 Cloud Field

4.4 Setup

The setup for simulating a shallow cumulus field is based on the LES intercomparison study by vanZanten et al. (2011), using their initial profiles for potential temperature and water vapor mixing ratio, the large-scale forcings, and surface fluxes. As in the original, the model domain covers an area of about $12.8\,\mathrm{km} \times 12.8\,\mathrm{km} \times 4.0\,\mathrm{km}$ in x-, y- and z-direction, respectively. The grid spacing is $\Delta x = \Delta y = 100\,\mathrm{m}$ in the horizontal, and $\Delta z = 40\,\mathrm{m}$ in the vertical. Moreover, the calculation of the domain-averaged quantities follows ~~(if possible)~~ the descriptions given in the original case.

Three different simulations will be presented. In the cases *LCM* N_P87 and *LCM* N_P400, the number of superdroplets per grid box are 87 and 400, respectively. With initial weighting factors of $A_{\mathrm{init}} = 1.89 \times 10^{12}$ and $A_{\mathrm{init}} = 7.0 \times 10^{12}$, respectively, these represent a CCN concentration of $100\,\mathrm{cm}^{-3}$ in each case. Moreover, one more simulation with splitting and merging is carried out. For this configuration, in which the general settings of *LCM* N_P87 are adopted, the splitting mode S with $r_{\mathrm{spl}} = 20\,\mu\mathrm{m}$, $\eta_{\mathrm{spl}} = 20$, and $A_{\mathrm{spl}} = \Delta x \times \Delta y \times \Delta z \times 1\,\mathrm{m}^{-3} = 4.0 \times 10^5$ is used. A_{spl} is chosen to allow number concentrations as small as $1\,\mathrm{m}^{-3}$ to be represent by a single superdroplet.

Based on the previously presented results, the maximum number of particles per grid box is set to $N_{\mathrm{P,max}} = 150$. Merging is applied in non-cloudy grid boxes for superdroplets with a radius smaller than $r_{\mathrm{mer}} = 0.1\,\mu\mathrm{m}$ and a weighting factor smaller than $A_{\mathrm{mer}} = A_{\mathrm{init}}/2$.

4.5 Cloud Field Results

The analysis is focused on the influence of splitting on the macroscopic properties of the shallow cumulus field. Figure 17 shows timeseries of (a) the LWP, (b) RWP, (c) ratio of the current superdroplet number to its initial value, (d) cloud cover (cc), (e) precipitation rate, and (f) total precipitation. Despite the superdroplet number, all these parameters agree in a statistical sense. In the cases without splitting, the total superdroplet number decreases slightly in the course of the simulation due

to precipitation (Fig. 17c), while the simulation with splitting increases the total superdroplet number by about 15%. Note, however, that both LWP and RWP are at the top of model variability documented in vanZanten et al. (2011) (gray areas), which is in line with the results of Arabas and Shima (2013), who also used an LCM for the simulation of this shallow cumulus case.

Considering the temporal variability of the precipitation rate and total precipitation (Fig. 17e and f), no significant changes are detectable using splitting or a very high number of superdroplets ~~in contrast to the single cloud simulations presented in the last section. This is foremost a result of the larger model domain alone, which attenuates variability simply by averaging~~. Nonetheless, a positive impact of splitting on the representation of precipitation can be seen in the probability density function of the surface precipitation rate (Fig. 18). For the simulation with 400 superdroplets per grid box and the splitting simulation, the probability for very high precipitation rates is smaller by about one order of magnitude compared to the simulation *LCM* N_P87. This clearly shows that extremely high precipitation rates, resulting from individual superdroplets with large weighting factors, are mitigated when splitting is applied. Accordingly, splitting is important for a statistical appropriate representation of individual rain events and necessary for the process-level understanding of the precipitation process, but the general features of the cloud field, as it was the case for the single cloud, are largely unaffected.

5 Conclusions

The main objective of this paper was the development and verification of a splitting algorithm to improve collisional growth in Lagrangian cloud models (LCMs). These models are able to represent collision and coalescence well (Unterstrasser et al., 2017; Dziekan and Pawlowska, 2017). Under certain conditions, however, they are known to insufficiently represented this process. These conditions occur when the number of superdroplets is low and, accordingly, the number of real droplets represented by each superdroplet (the so-called weighting factor) is high, leading to an oversimplified representation of the droplet size distribution (DSD) (Riechelmann et al., 2012; Unterstrasser et al., 2017). The introduced approach for splitting is carried out by cloning superdroplets of interest (large radius and high weighting factor) into a large number of identical superdroplets with commensurately reduced weighting factors, which improves the representation of the DSD in the desired areas. An accompanying merging algorithm has been also introduced. It is designed to merge two superdroplets into one, counteracting the (potentially) massive production of superdroplets due to splitting and hence a significant increase of computational costs.

The splitting and merging algorithms have been validated using box-simulations, a simulation of a single cumulus cloud, and an established shallow cumulus test case. The box-simulations confirmed that the capability of an LCM to represent the temporal evolution of a DSD due to collision and coalescence depends crucially on the number of simulated superdroplets (Shima et al., 2009; Riechelmann et al., 2012; Unterstrasser et al., 2017; Dziekan and Pawlowska, 2017). Without splitting, only simulations with more than 500 to 1000 superdroplets per grid box were acceptably reproducing literature references. By applying the new splitting algorithm, the results improved significantly using only up to 150 superdroplets per grid-box. Furthermore, the box-simulations revealed that the radius from which splitting is applied is the most important parameter of the splitting algorithm. A value of $15\,\mu\mathrm{m}$, which corresponds to the typical radii of the first colliding droplets in clouds, was

found to be appropriate. Other investigated parameters have shown only a minor impact on the results as long as a sufficiently large maximum number of superdroplets is allowed to be produced by splitting (≥ 150).

In the idealized single cloud simulation, splitting improved the representation of collisional growth with up to 70 % larger maximum radii ~~and a slight increase of the rain water path of up to 12 %~~. Moreover, splitting improves the spatial and temporal representation of precipitation by distributing the precipitable water on more superdroplets with an accordingly smaller weighting factors. It is important to note, however, that the life cycle and domain-averaged macroscopic properties are almost not affected by the splitting process. If applied, the merging algorithm has been shown to reduce the computing time by 18% and the storage demand at least by 7% in comparison to simulations with splitting alone. Since merging is restricted to cloud-free regions, its application did not alter the simulated physics. Similar findings on the effect of splitting on the production of rain have been made for the shallow cumulus test case.

In the light of the fact that LCMs become increasingly important in the field of modeling cloud microphysics, it is necessary to minimize the (typically) large demand of memory and computing time required for their application. Thus, a fixed number of superdroplets needs to be replaced by a dynamic number, which adapts interactively to the given physical and numerical requirements. In this regard, the presented methods follow the approaches by Grabowski et al. (2018), in which superdroplets are only created after activation, or Naumann and Seifert (2015), who restricted the superdroplet approach to the representation of raindrops. Of course, all these approaches have their specific advantages and disadvantages, but they are necessary steps to apply LCMs in a wider range of future applications.

Code availability. The LES model used in this study (revision 2263) is publicly available on https://palm.muk.uni-hannover.de/trac/browser/palm?rev=2263. For analysis, the model has been extended and additional analysis tools have been developed. The extended code is available from the authors on request.

Acknowledgements. All simulations have been carried out on the Cray XC-40 systems of the North-German Supercomputing Alliance (HLRN, https://www.hlrn.de/). The publication of this article was funded by the Open Access fund of Leibniz Universität Hannover.

References

Andrejczuk, M., Grabowski, W., Reisner, J., and Gadian, A.: Cloud-aerosol interactions for boundary layer stratocumulus in the Lagrangian Cloud Model, J. Geophys. Res., 115, 2010.

Arabas, S. and Shima, S.-i.: Large-eddy simulations of trade wind cumuli using particle-based microphysics with Monte Carlo coalescence, J. Atmos. Sci., 70, 2768–2777, 2013.

Arabas, S., Jaruga, A., Pawlowska, H., and Grabowski, W. W.: libcloudph++ 1.0: a single-moment bulk, double-moment bulk, and particle-based warm-rain microphysics library in C++, Geosci. Model Dev., 8, 1677–1707, 2015.

Dziekan, P. and Pawlowska, H.: Stochastic coalescence in Lagrangian cloud microphysics, Atmos. Chem. Phys., 17, 13 509–13 520, 2017.

Grabowski, W. W., Dziekan, P., and Pawlowska, H.: Lagrangian condensation microphysics with Twomey CCN activation, Geosci. Model Dev., 11, 103, 2018.

Hall, W. D.: A detailed microphysical model within a two-dimensional dynamic framework: Model description and preliminary results, J. Atmos. Sci., 37, 2486–2507, 1980.

Hoffmann, F.: On the limits of Köhler activation theory: how do collision and coalescence affect the activation of aerosols?, Atmos. Chem. Phys., 17, 8343–8356, 2017.

Hoffmann, F., Raasch, S., and Noh, Y.: Entrainment of aerosols and their activation in a shallow cumulus cloud studied with a coupled LCM-LES approach, Atmos. Res., 156, 43–57, 2015.

Hoffmann, F., Noh, Y., and Raasch, S.: The route to raindrop formation in a shallow cumulus cloud simulated by a Lagrangian cloud model, J. Atmos. Sci., 74, 2125–2142, 2017.

Maronga, B., Gryschka, M., Heinze, R., Hoffmann, F., Kanani-Sühring, F., Keck, M., Ketelsen, K., Letzel, M. O., Sühring, M., and Raasch, S.: The Parallelized Large-Eddy Simulation Model (PALM) version 4.0 for atmospheric and oceanic flows: model formulation, recent developments, and future perspectives, Geosci. Model Dev., 8, 2515–2551, 2015.

Naumann, A. K. and Seifert, A.: A Lagrangian drop model to study warm rain microphysical processes in shallow cumulus, J. Adv. Model. Earth Syst., 7, 1136–1154, 2015.

Naumann, A. K. and Seifert, A.: Recirculation and growth of raindrops in simulated shallow cumulus, J. Adv. Model. Earth Syst., 8, 520–537, 2016.

Riechelmann, T., Noh, Y., and Raasch, S.: A new method for large-eddy simulations of clouds with Lagrangian droplets including the effects of turbulent collision, New J. Phys., 14, 065 008, 2012.

Rogers, R. R. and Yau, M. K.: A Short Course in Cloud Physics, Pergamon Press, New York, 1989.

Sardina, G., Poulain, S., Brandt, L., and Caballero, R.: Broadening of Cloud Droplet Size Spectra by Stochastic Condensation: Effects of Mean Updraft Velocity and CCN Activation, J. Atmos. Sci., 75, 451–467, 2018.

Seifert, A.: On the parameterization of evaporation of raindrops as simulated by a one-dimensional rainshaft model, J. Atmos. Sci., 65, 3608–3619, 2008.

Shaw, R. A., Reade, W. C., Collins, L. R., and Verlinde, J.: Preferential concentration of cloud droplets by turbulence: Effects on the early evolution of cumulus cloud droplet spectra, J. Atmos. Sci., 55, 1965–1976, 1998.

Shima, S., Kusano, K., Kawano, A., Sugiyama, T., and Kawahara, S.: The super-droplet method for the numerical simulation of clouds and precipitation: A particle-based and probabilistic microphysics model coupled with a non-hydrostatic model, Quart. J. Roy. Meteor. Soc., 135, 1307–1320, 2009.

Sölch, I. and Kärcher, B.: A large-eddy model for cirrus clouds with explicit aerosol and ice microphysics and Lagrangian ice particle tracking, Quart. J. Roy. Meteor. Soc., 136, 2074–2093, 2010.

Ulbrich, C. W.: Natural variations in the analytical form of the raindrop size distribution, J. Climate Appl. Meteor., 22, 1764–1775, 1983.

Unterstrasser, S. and Sölch, I.: Optimisation of the simulation particle number in a Lagrangian ice microphysical model, Geosci. Model Dev., 7, 695–709, 2014.

Unterstrasser, S., Hoffmann, F., and Lerch, M.: Collection/aggregation algorithms in Lagrangian cloud microphysical models: rigorous evaluation in box model simulations, Geosci. Model Dev., 10, 1521–1548, 2017.

vanZanten, M. C., Stevens, B., Nuijens, L., Siebesma, A. P., Ackerman, A. S., Burnet, F., Cheng, A., Couvreux, F., Jiang, H., Khairoutdinov, M., Kogan, Y., Lewellen, D. C., Mechem, D., Nakamura, K., Noda, A., Shipway, B. J., Slawinska, J., Wang, S., and Wyszogrodzki, A.: Controls on precipitation and cloudiness in simulations of trade-wind cumulus as observed during RICO, J. Adv. Model. Earth Syst., 3, 2011.

Wang, L.-P., Xue, Y., and Grabowski, W. W.: A bin integral method for solving the kinetic collection equation, J. Comput. Phys., 226, 59–88, 2007.

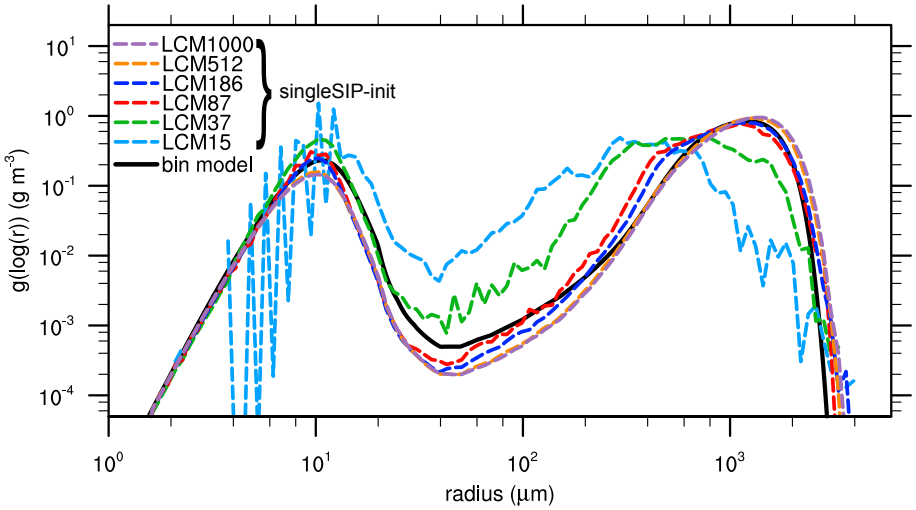

Figure 1. Mass density distribution for the single-box approach after 3600 s for the singleSIP-initialization. The black solid line denotes the solution of Wang et al. (2007). The colored dashed curves show the solution of the LCM with different numbers of superdroplets per grid box.

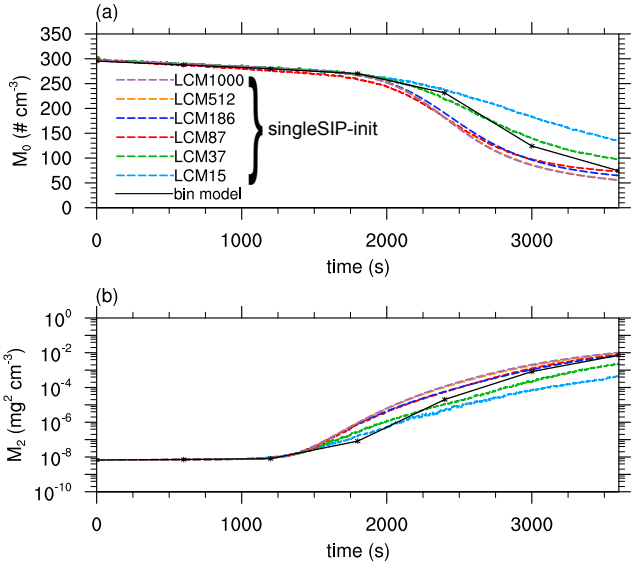

Figure 2. Moments of the mass density distribution as a function of time obtained from the single-box simulations for the singleSIP-initialization. The black solid line denotes the solution of Wang et al. (2007). The colored dashed curves show the solution of the LCM with different numbers of superdroplets per grid box.

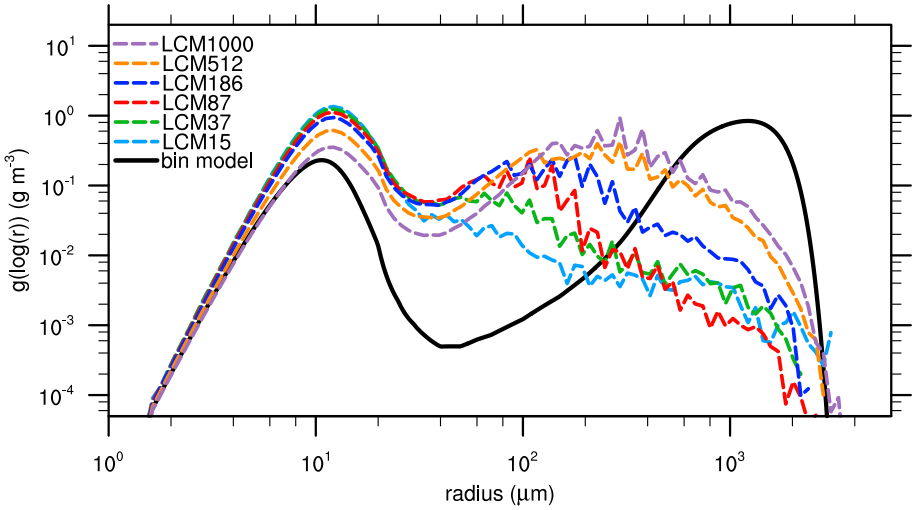

Figure 3. Mass density distribution for the single-box approach after 3600 s. The black solid line denotes the solution of Wang et al. (2007). The colored dashed curves show the solution of the LCM with different numbers of superdroplets per grid box.

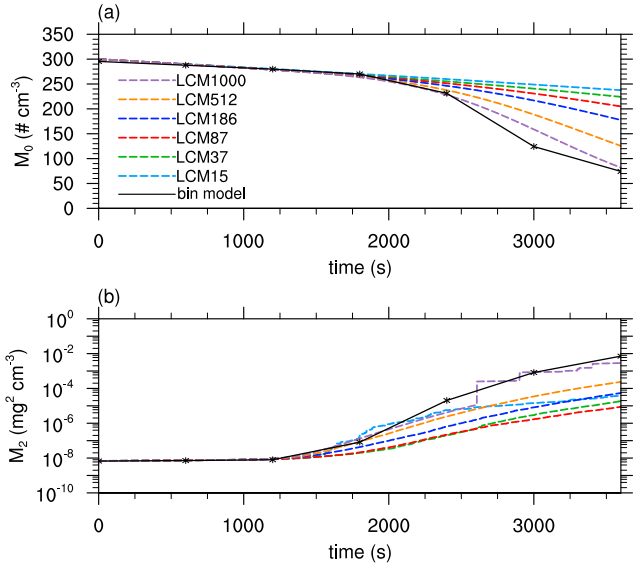

Figure 4. Moments of the mass density distribution as a function of time obtained from the single-box simulations. The black solid line denotes the solution of Wang et al. (2007). The colored dashed curves show the solution of the LCM with different numbers of superdroplets per grid box.

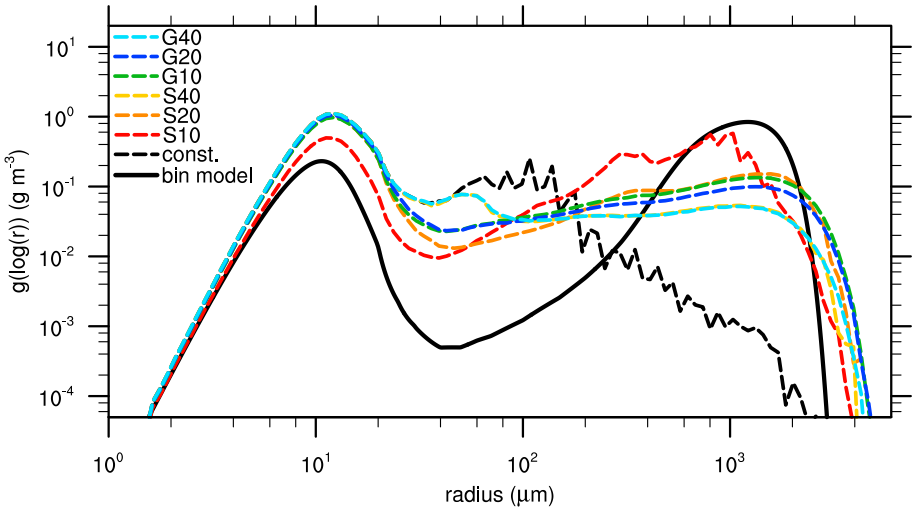

Figure 5. Mass density distribution for the single-box approach after 3600 s. The black solid line denotes the solution of Wang et al. (2007), the black dashed curve the reference case (without splitting). The colored dashed curves show solution for splitting simulation with different configurations.

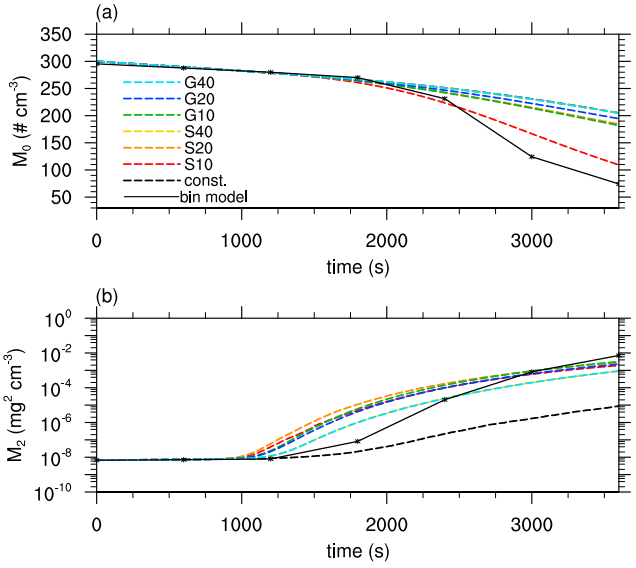

Figure 6. Moments of the mass density distribution as a function of time obtained from single-box simulations. The black solid line denotes the solution of Wang et al. (2007), the black dashed curve for the reference simulation (without splitting). The colored dashed curves show the solutions for different splitting configurations.

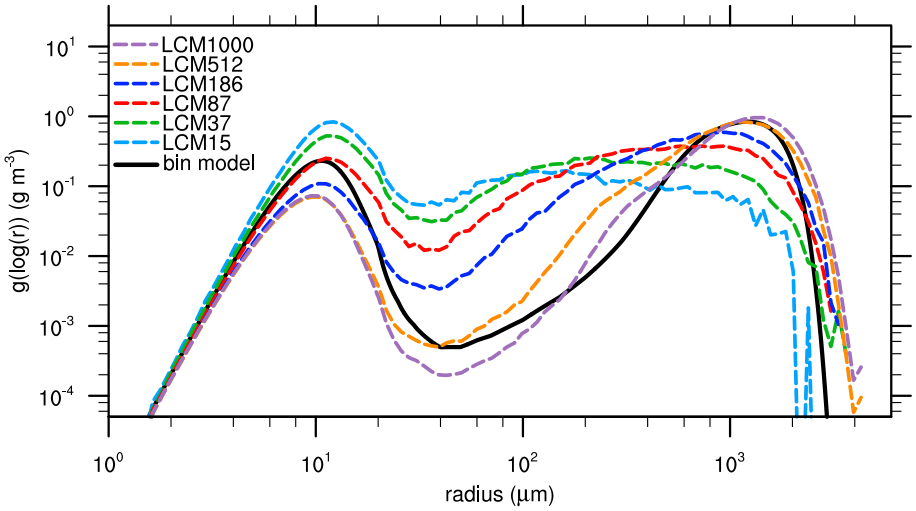

Figure 7. Same as Fig. 3 but for the multi-box approach, i.e. interactions between the grid boxes are possible.

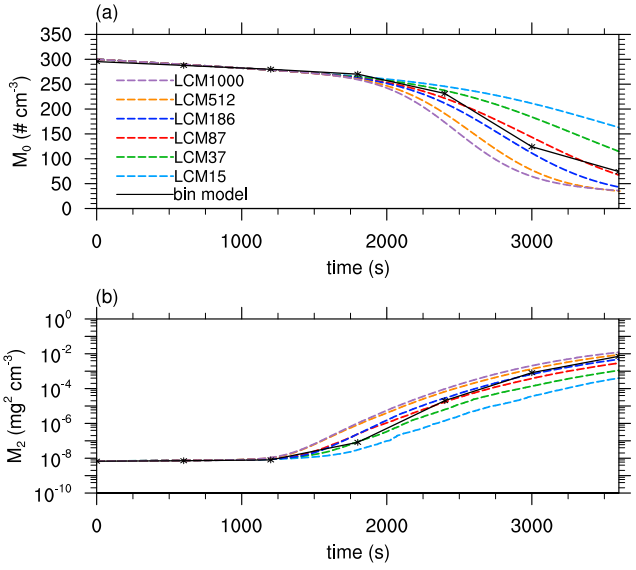

Figure 8. Same as Fig. 4 but for the multi-box approach, i.e. interactions between the grid boxes are possible.

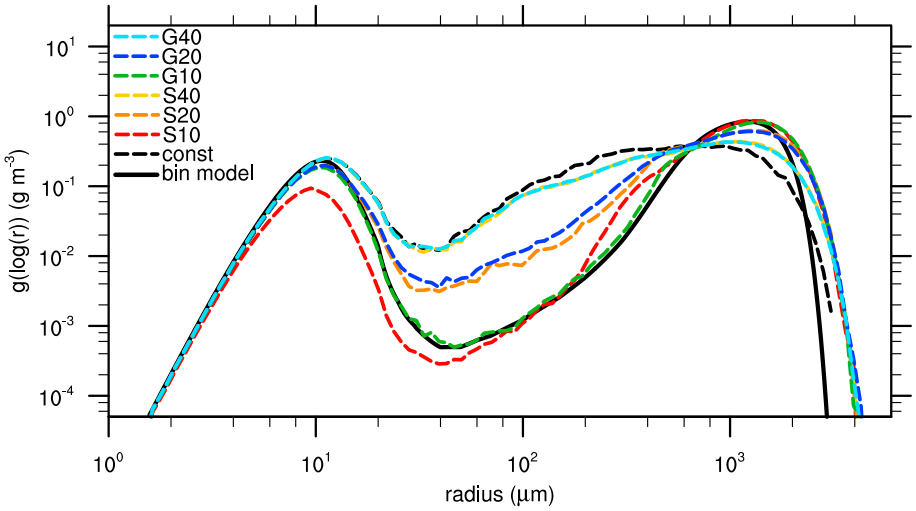

Figure 9. Same as Fig. 5 but for the multi-box approach, i.e. interactions between the grid boxes are possible.

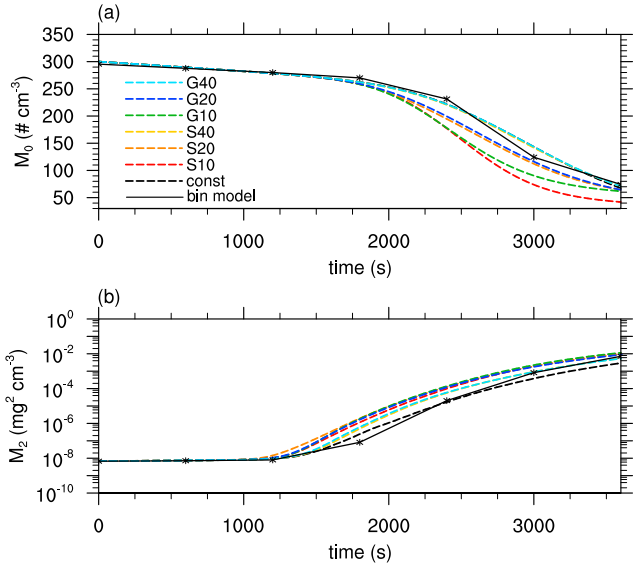

Figure 10. Same as Fig. 6 but for the multi-box approach, i.e. interactions between the grid boxes are possible.

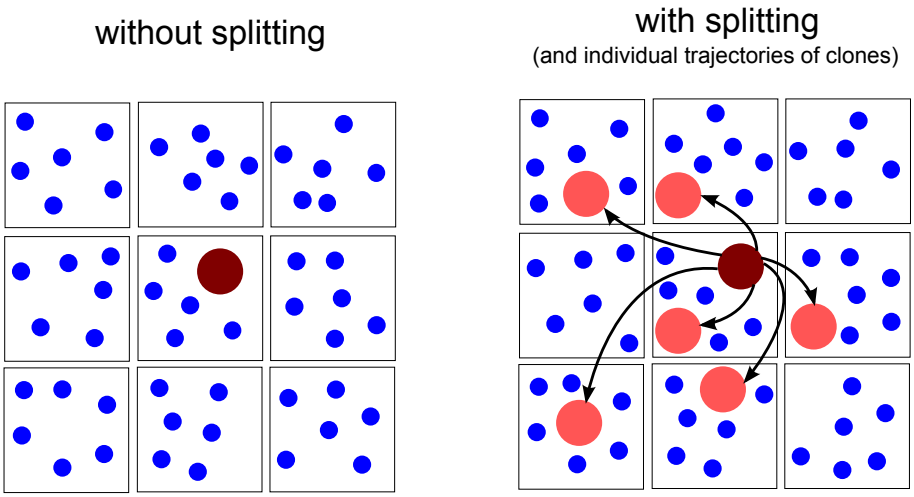

Figure 11. Schematic representation on how splitting affects the spatial distribution of large superdroplets. The squares outline the different grid boxes with superdroplets of the size of cloud droplets (blue) and superdroplets representing rain drops (dark red). Without splitting (left), the rain drop is represented by only one superdroplet. In the splitting case with multi-box approach, this superdroplet is cloned into several superdroplets, which are able to move in other grid boxes (due to their individual SGS-velocities) where they initiate or affect collisional growth.

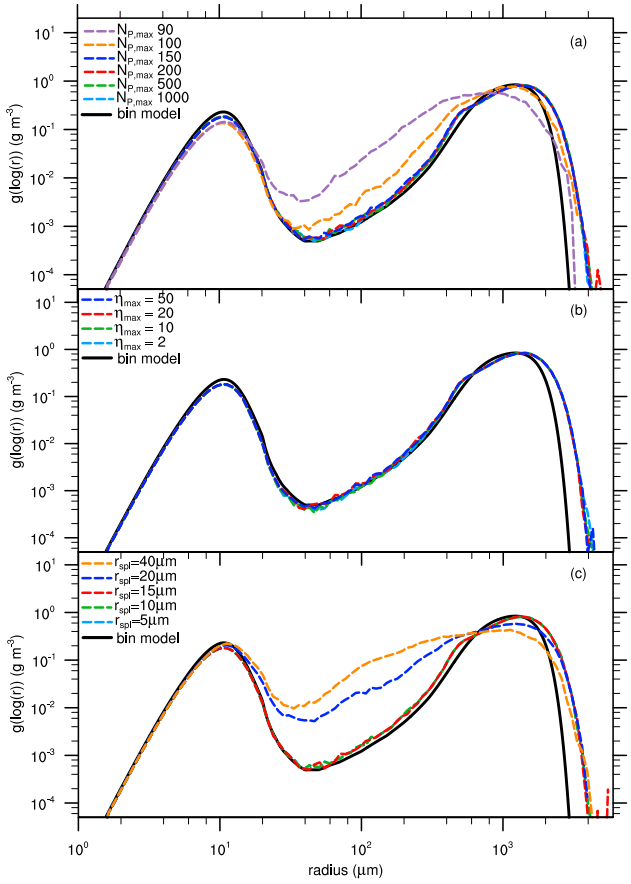

Figure 12. Mass density distribution for the box-simulation after 3600 s. The black solid line denotes the solution of Wang et al. (2007). In (a), sensitivity studies for different values of $N_{\mathrm{P,max}}$ are presented. In (b), simulations for different values of η_{max} are shown. In (c), results for different splitting radii are displayed. All Sensitivity studies are conducted using the splitting mode G.

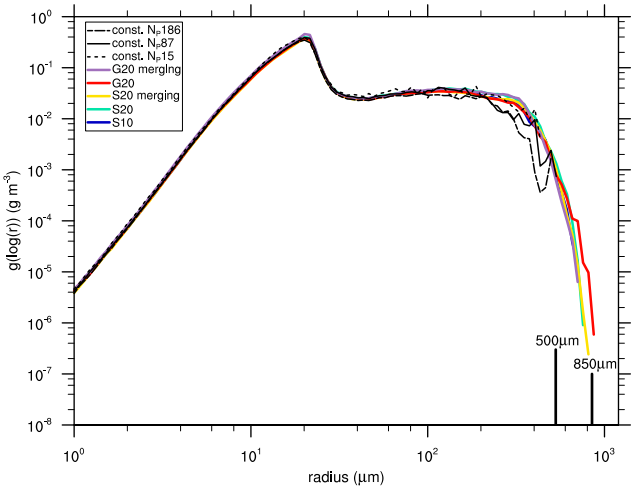

Figure 13. Mass density distribution after 1800 s for the idealized single cloud simulations using parameters described in Tab.1.

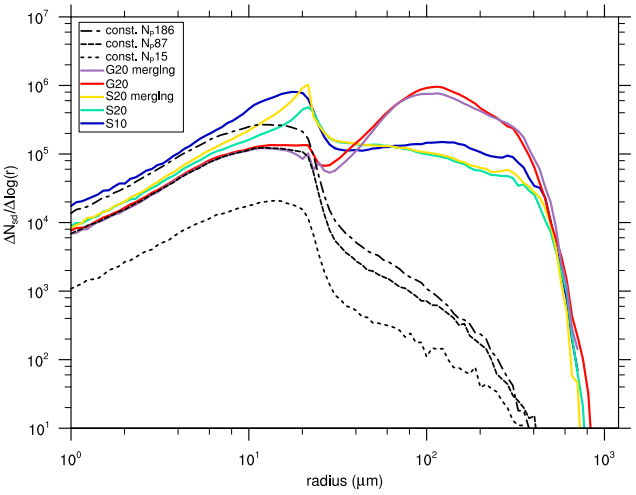

Figure 14. Total number of superdroplets per logarithmic radius bin after t = 1800 s for the idealized single cloud simulations using parameters described in Tab.1.

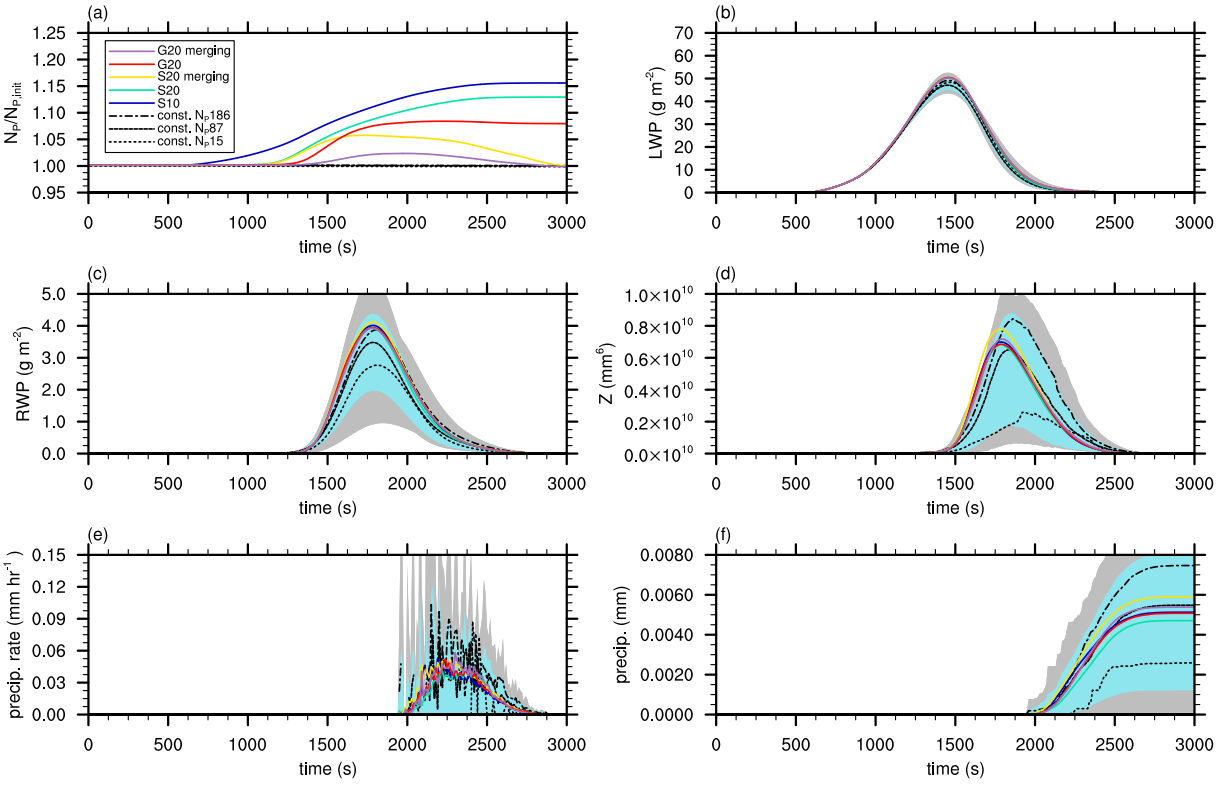

Figure 15. Timeseries of different variables for the idealized single cloud simulation for different initial numbers of superdroplets and splitting configurations. In (a), the ratio of the actual and initialized number of superdroplets in the whole model domain is shown. The liquid water path (LWP) and rainwater path (RWP) are displayed in panels (b) and (c), respectively. In (d), the total radar reflectivity is shown. Panels (e) and (f) show the precipitation rate and total precipitation, respectively. The reference simulations (runs without splitting) are presented as a mean of five ensembles for each case. Moreover, the light blue areas show the mean plus-minus one standard deviation and the gray areas show the range derived from all 15 ensemble members.

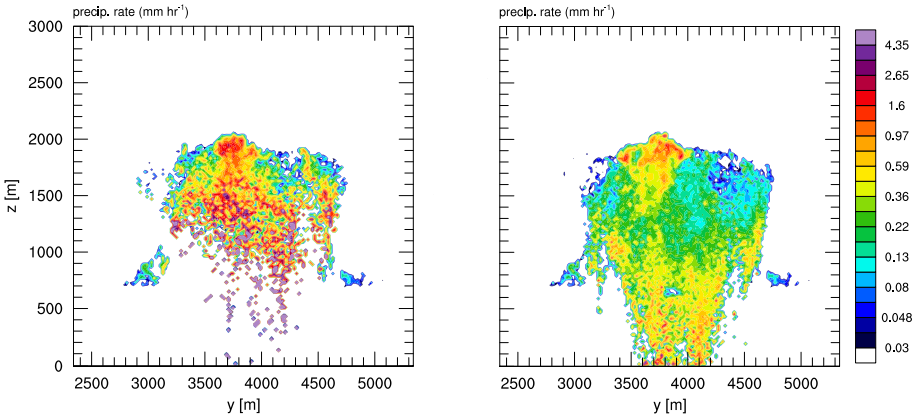

Figure 16. Vertical cross-sections of the precipitation rate for the reference case (left) and the splitting case *S20* (right).

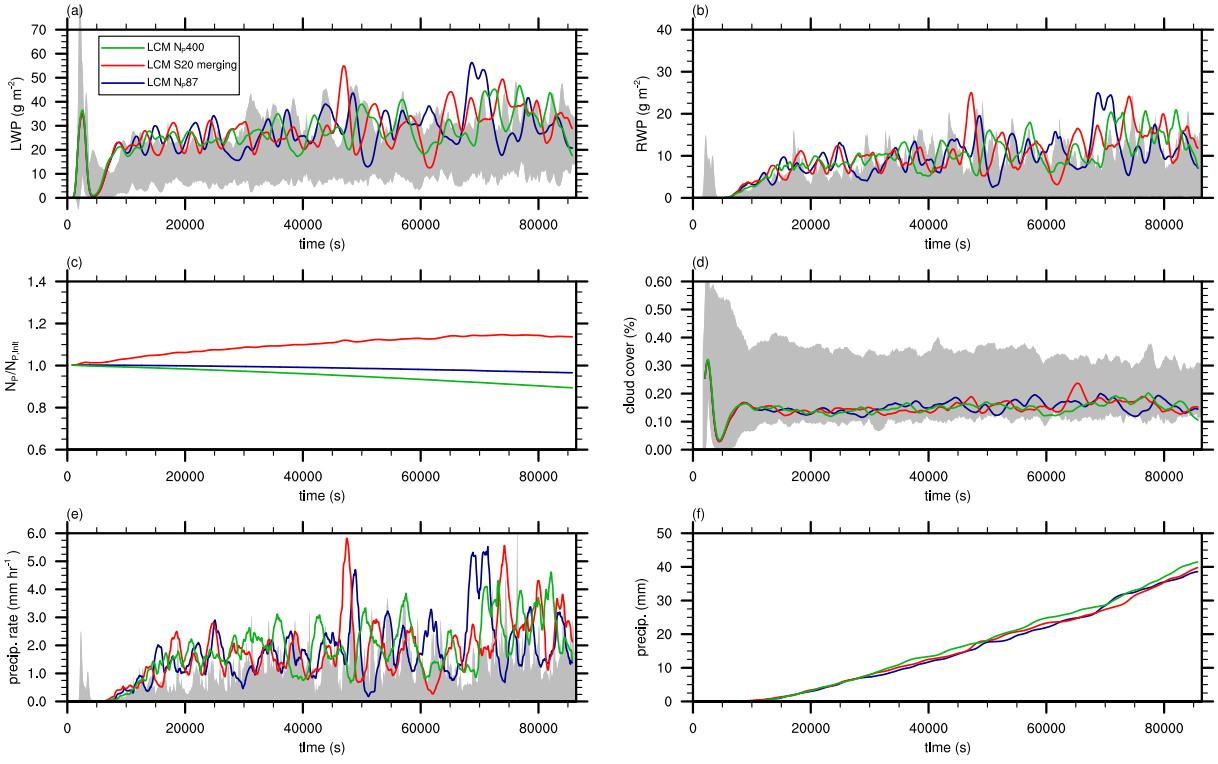

Figure 17. Timeseries of (a) the liquid water path (LWP), (b) rainwater path (RWP), (c) ratio of the actual number of superdroplets to the initial number of superdroplets, (d) cloud cover, (e) precipitation rate, and (f) total precipitation for different initial numbers of superdroplets and splitting configurations. The gray areas in (a), (b) and (d) indicate the documented model variability of the simulated shallow cumulus case (vanZanten et al., 2011).

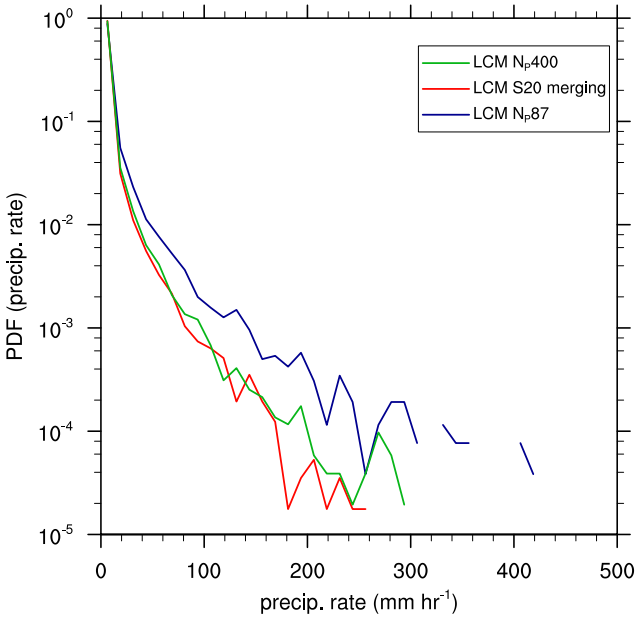

Figure 18. Probability density function of precipitation rates for different initial numbers of superdroplets and splitting configurations.